



2014

High Fidelity Chemistry And Radiation Modeling For Oxy-Combustion Scenarios

Hassan A. Abdul Sater

Follow this and additional works at: <https://commons.und.edu/theses>



Part of the [Chemical Engineering Commons](#)

Recommended Citation

Abdul Sater, Hassan A., "High Fidelity Chemistry And Radiation Modeling For Oxy-Combustion Scenarios" (2014). *Theses and Dissertations*. 417.

<https://commons.und.edu/theses/417>

This Thesis is brought to you for free and open access by the Theses, Dissertations, and Senior Projects at UND Scholarly Commons. It has been accepted for inclusion in Theses and Dissertations by an authorized administrator of UND Scholarly Commons. For more information, please contact zeinebyousif@library.und.edu.

HIGH FIDELITY CHEMISTRY AND RADIATION
MODELING FOR OXY – COMBUSTION
SCENARIOS

by

Hassan A Abdul Sater
Bachelor of Science, California State Polytechnic University – Pomona, 2011

A Thesis

Submitted to the Graduate Faculty

of the

University of North Dakota

in partial fulfillment of the requirements

for the degree of

Master of Science

Grand Forks, North Dakota
August
2014

Copyright © 2014 Hassan A Abdul Sater


This thesis, submitted by Hassan A Abdul Sater in partial fulfillment of the requirements for the Degree of Master of Science from the University of North Dakota, has been read by the Faculty Advisory Committee under whom the work has been done and is hereby approved.



Dr. Gautham Krishnamoorthy, Chairperson




Dr. Frank Bowman

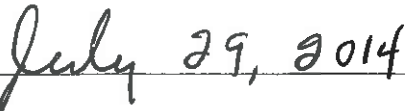


Dr. Steven Benson

This thesis is being submitted by the appointed advisory committee as having met all of the requirements of the School of Graduate Studies at the University of North Dakota and is hereby approved.



Wayne Swisher, Dean of the School of Graduate Studies



Date

PERMISSION

Title High Fidelity Chemistry and Radiation Modeling for Oxy-Combustion Scenarios

Department Chemical Engineering

Degree Master of Science

In presenting this thesis in partial fulfillment of the requirements for a graduate degree from the University of North Dakota, I agree that the library of this University shall make it freely available for inspection. I further agree that permission for extensive copying for scholarly purposes may be granted by the professor who supervised my thesis work or, in her absence, by the Chairperson of the department or the dean of the School of Graduate Studies. It is understood that any copying or publication or other use of this thesis or part thereof for financial gain shall not be allowed without my written permission. It is also understood that due recognition shall be given to me and to the University of North Dakota in any scholarly use which may be made of any material in my thesis.

Hassan A Abdul Sater

July 2014

TABLE OF CONTENTS

LIST OF TABLES.....	ix
LIST OF FIGURES	x
Nomenclature	xiii
Acknowledgements	xv
Abstract.....	xvi
1. Introduction.....	1
1.1. Carbon Capture Technology.....	1
1.2. Oxy-fuel Combustion	2
1.2.1. Diffusion Oxy-methane Flames.....	3
1.3. Numerical Modeling.....	3
1.3.1. Radiative Heat Transfer	4
1.3.2. Chemistry.....	4
1.4. Thesis Outline.....	5
1.5. References.....	6
2. An Assessment of Radiation Modeling Strategies in Simulations of Laminar to Transitional, Oxy-Methane, Diffusion Flames.....	8
2.1. Introduction.....	9
2.1.1. Numerical Modeling of oxy-fuel combustion.....	9
2.1.2. Motivation for the Present Study	11
2.2. Laminar to Transitional, Oxy-Methane, Diffusion Flames	11

2.3.	CFD Modeling Approach	12
2.3.1.	Geometry and Mesh	12
2.3.2.	Radiation Modeling and Boundary Conditions	13
2.3.3.	Chemistry Modeling	17
2.4.	Results and Discussion	18
2.4.1.	Temperature and Flame Lengths.....	18
2.4.2.	Radiant Fraction Predictions.....	25
2.4.3.	Effects of Soot Model	31
2.4.4.	Turbulence Radiation Interaction (TRI) Model	35
2.5.	Conclusions.....	37
2.6.	References.....	39
3.	An Experimental and Numerical Study of Confined, Laminar, Diffusion, Oxy-Methane Flames.....	44
3.1.	Introduction.....	45
3.1.1.	Oxy-methane combustion chemistry	45
3.2.	Experimental Conditions	48
3.3.	CFD Modeling Approach	49
3.3.1.	Geometry and Mesh	49
3.3.2.	Radiation Modeling and Boundary Conditions	51
3.3.3.	Chemistry Modeling	52
3.4.	Results and Discussion	54
3.4.1.	Temperature	54
3.4.2.	CO ₂	58
3.4.3.	O ₂	60

3.4.4.	CO	60
3.4.5.	OH and Flame Lengths	63
3.4.6.	Soret Effect	66
3.5.	Conclusions.....	68
3.6.	References.....	71
4.	Predicting Radiative Heat Transfer in Oxy-Methane Flame Simulations: An Examination of its Sensitivities to Chemistry and Radiative Property Models	75
4.1.	Introduction.....	76
4.1.1.	Chemistry and Radiative Heat Transfer in Oxy-Methane Combustion.....	76
4.1.2.	Assessing the Accuracies of Radiative Transfer Predictions: Current Needs.....	77
4.2.	Experimental Conditions	81
4.3.	CFD Modeling Approach	81
4.3.1.	Mesh and Flow Modeling	81
4.3.2.	Radiation Modeling and Boundary Conditions	81
4.3.3.	Chemistry Modeling	82
4.4.	Results and Discussion	82
4.4.1.	Wall Incident Radiative Fluxes.....	82
4.4.2.	Directional Radiative Flux Predictions from RADCAL.....	85
4.4.3.	Effect of WSGGM Spectroscopic/Model Database.....	89
4.5.	Conclusions.....	92
4.6.	References.....	94
5.	Conclusions.....	97
5.1.	Summary of Results.....	97

5.2. Future Work 99

LIST OF TABLES

Table	Page
2-1: Percent variation between the numerical predictions of the flame length and the experimental values for the gray and non-gray models.	24
2-2: Percentage deviation of the gray model estimates of the radiant fraction from the corresponding non-gray radiant fraction estimates.	31
3-1: A summary of previous CFD studies of oxy-methane/natural gas combustion.	47
4-1: A summary of WSGGM investigated in this study.	82
4-2: Volume integrated radiative source (in W) (Q_R) for the different flames investigated in this study.	90

LIST OF FIGURES

Figure	Page
2-1: Temperature profiles predicted along the height of the wall for: (a) Methane-Air flames at different fuel inlet Reynolds numbers; (b) Methane-Air flames and oxy-methane flames at fuel inlet Reynolds numbers of 468 and 2340.	16
2-2: Temperature contours (in K) within the reactor at different oxidizer compositions: a) air, b) 40% O ₂ in CO ₂ , c) 70% O ₂ in CO ₂	20
2-3: Radial temperature profiles at different axial locations within the reactor for the Oxy-methane flame (Re 1404; 35% O ₂ - 65% CO ₂ oxidizer composition). CFD predictions are with the non-gray WSGGM.	21
2-4: Radial temperature profiles at different axial locations within the reactor for the oxy-methane flame (Re 1404; 35% O ₂ - 65% CO ₂ oxidizer composition). Gray versus non-gray model comparisons.	22
2-5: Flame length predictions employing gray and non-gray models as a function of oxygen compositions in the oxidizer and fuel inlet Reynolds numbers.	24
2-6: Predictions of the axial variations in the OH mole fractions in different flames.	25
2-7: Temperature profiles predicted along the height of the wall employing gray and non-gray radiation models for: (a) Methane-Air flames; (b) Oxy-methane flames (70% O ₂).	26
2-8: Radiant fraction loss predictions employing gray and non-gray models at various oxidizer compositions and Reynolds numbers.	30
2-9: Soot volume fraction predictions employing the non-gray model at Reynolds number 468 and 2340 for several oxidizer compositions.	33
2-10: Effect of soot on the radiant fraction at Re 468 and Re 2340.	34
2-11: Emission enhancement due to TRI in different flames.	37
3-1: Radial temperature profiles at different axial locations for the air-methane flame.	56

3-2: Radial temperature profiles at different axial locations for the Oxy-methane flame (35% O ₂ - 65% CO ₂).	57
3-3: Radial temperature profiles at different axial locations for the Oxy-methane flame (50 % O ₂ - 50% CO ₂).	57
3-4: Radial CO ₂ profiles at different axial locations for the air-methane flame.	58
3-5: Radial CO ₂ profiles at different axial locations for the oxy-methane flame (35% O ₂ - 65% CO ₂).	59
3-6: Radial CO ₂ profiles at different axial locations for the oxy-methane flame (50 % O ₂ - 50% CO ₂).	59
3-7: Radial O ₂ profiles at different axial locations for the air and oxy-flames investigated in this study.	60
3-8: Radial CO profiles at different axial locations for the air and oxy-flames investigated in this study.	62
3-9: Axial CO profiles for the air and oxy-flames investigated in this study.	63
3-10: Axial OH profiles for the air and oxy-flames investigated in this study.	65
3-11: The sensitivity of flame length predictions to the choice of chemistry model for the air and oxy-flames investigated in this study.	65
3-12: Axial O profiles for the air and oxy-flames investigated in this study.	66
3-13: Axial CO, OH and temperature variations in the three flames in the EDC model calculations with and without accounting for Soret effect in the calculations.	68
4-1: Variations in the incident radiative fluxes (in W/m ²) at the wall predicted by the different chemistry models (the wall averaged percentage variations between the models are indicated near circled regions).	84
4-2: Directional radiative flux predictions from RADCAL at different heights along the furnace wall in the air and oxy-flames flames (Re 1404). Open symbols correspond to predictions where CO, CH ₄ radiation was not accounted for in the calculations.	87
4-3: Percentage reduction in the directional radiative flux when not accounting for CO, CH ₄ contributions to radiative transfer in calculations performed with mixture fraction based chemistry model (unless indicated in the legends) and Perry (5gg) WSGGM: (a) Re 468; (b) Re 1404; (c) Re 2340.	88

4-4: Variations in the incident radiative fluxes (in W/m²) at the wall predicted by the different WSGG models (the maximum of the wall averaged percentage variations between the models are indicated near circled regions).....91

NOMENCLATURE

Abbreviations

CCS	Carbon Capture and Storage
CFD	Computational Fluid Dynamics
DO	Discrete Ordinate model
EDC	Eddy Dissipation Concept
EIA	Energy Information Administration
EWBM	Exponential Wide Band Model
FR	Finite Rate
gg	Gray Gas
JL	Jones-Lindstedt
LBL	Line by Line
PDF	Probability Density Function
ppmv	Parts Per Million Volume
Re	Reynolds Number
RTE	Radiative Transfer Equation
SNB	Statistical Narrow Band
TRI	Turbulence-Radiation Interactions
UDF	User Defined Function
WD	Westbrook Dryer
WSGGM	Weighted Sum of Gray Gases Model

Chemical Species

C(s)	Carbon
C ₂ H ₂	Ethyne
C ₂ H ₄	Ethylene
C ₂ H ₆	Ethane
C ₂ N ₂	Cyanogen
C ₃ H ₃	Propynyl
C ₄ H ₂	Diacetylene
CH ₃	Methyl
CH ₄	Methane
CO	Carbon Monoxide
CO ₂	Carbon Dioxide
H	Hydrogen atom
H ₂	Hydrogen

H ₂ O	Water
HNC	Hydredrogen Isocyanide
HO ₂	Hydroperoxyl
N ₂	Nitrogen
NO _x	Nitric Oxides
O	Oxygen atom
OH	Hydroxyl
SO _x	Sulfur Oxides

Symbols

k	Absorption coefficient
G	Total incident radiation
I	Radiation Intensity
I _b	Black body emissivity
i	Band
q	Heat Flux
Q _R	Radiant source
r	Radius
Ω	Solid Angle

ACKNOWLEDGEMENTS

Words can never adequately express my sincere appreciation and gratitude for Dr. Gautham Krishnamoorthy for training, teaching and coaching me while working on this thesis. I cannot thank you enough for the vast patience and tremendous support you have provided me with during my studies at UND. Your limitless dedication, provision and enthusiasm towards scientific research are truly inspirational.

I want to also express gratitude for my committee members Dr. Steve Benson and Dr. Frank Bowman for their time and assistance with this thesis. My sincere appreciation also goes to Dr. Mario Ditaranto for contributing to this thesis by allowing us to publish his experimental data and for his invaluable assistance. I am very grateful to my colleague Ms. Caitlyn Wolf for her contributions at various stages of this thesis.

I would also like to thank the UND Chemical Engineering department staff and my fellow graduate students for facilitating the completion of this thesis. Lastly, I want to thank my brothers, sisters and parents who have always been a great source of motivation and inspiration. Your support and selfless love have strengthened me and provided me with the encouragement necessary to accomplish this thesis.

Hassan A Abdul Sater

ABSTRACT

To account for the thermal and chemical effects associated with the high CO₂ concentrations in an oxy-combustion atmosphere, several refined gas-phase chemistry and radiative property models have been formulated for laminar to highly turbulent systems. This thesis examines the accuracies of several chemistry and radiative property models employed in computational fluid dynamic (CFD) simulations of laminar to transitional oxy-methane diffusion flames by comparing their predictions against experimental data. Literature review about chemistry and radiation modeling in oxy-combustion atmospheres considered turbulent systems where the predictions are impacted by the interplay and accuracies of the turbulence, radiation and chemistry models. Thus, by considering a laminar system we minimize the impact of turbulence and the uncertainties associated with turbulence models.

In the first section of this thesis, an assessment and validation of gray and non-gray formulations of a recently proposed weighted-sum-of-gray gas model in oxy-combustion scenarios was undertaken. Predictions of gas, wall temperatures and flame lengths were in good agreement with experimental measurements. The temperature and flame length predictions were not sensitive to the radiative property model employed. However, there were significant variations between the gray and non-gray model radiant fraction predictions with the variations in general increasing with decrease in Reynolds numbers possibly attributed to shorter flames and steeper temperature gradients. The results of this section

confirm that non-gray model predictions of radiative heat fluxes are more accurate than gray model predictions especially at steeper temperature gradients.

In the second section, the accuracies of three gas-phase chemistry models were assessed by comparing their predictions against experimental measurements of temperature, species concentrations and flame lengths. The chemistry was modeled employing the Eddy Dissipation Concept (EDC) employing a 41-step detailed chemistry mechanism, the non-adiabatic extension of the equilibrium Probability Density Function (PDF) based mixture-fraction model and a two-step global finite rate chemistry model with modified rate constants proposed to work well in oxy-methane flames. Based on the results from this section, the equilibrium PDF model in conjunction with a high-fidelity non-gray model for the radiative properties of the gas-phase may be deemed as accurate to capture the major gas species concentrations, temperatures and flame lengths in oxy-methane flames.

The third section examines the variations in radiative transfer predictions due to the choice of chemistry and gas-phase radiative property models. The radiative properties were estimated employing four weighted-sum-of-gray-gases models (WSGGM) that were formulated employing different spectroscopic/model databases. An average variation of 14 – 17% in the wall incident radiative fluxes was observed between the EDC and equilibrium mixture fraction chemistry models, due to differences in their temperature predictions within the flame. One-dimensional, line-of-sight radiation calculations showed a 15 – 25 % reduction in the directional radiative fluxes at lower axial locations as a result of ignoring radiation from CO and CH₄. Under the constraints of fixed temperature and species distributions, the flame radiant power estimates and average wall incident radiative fluxes varied by nearly 60% and 11% respectively among the different WSGG models.

1. INTRODUCTION

1.1. Carbon Capture Technology

The EIA projected in 2013 that renewable energy fuels and natural gas will be the fastest growing forms of energy in terms of world electricity generation [1]. Coal on the other hand is projected to hold the largest share of the world's electricity generation in 2040. Despite the fact that renewable energy are continuing to rise in terms of power generation, fossil fuels are still responsible for generating about 55% of world's power. This means that carbon dioxide released into the atmosphere will also increase.

Carbon dioxide is the major contributor to global warming for it has the greatest impact which accounts to about 55% of the observed global warming and 65% of the enhanced greenhouse effect [2]. The intergovernmental Panel on Climate Control predicted that by the year 2100, the atmosphere may contain about 570 ppmv of CO₂ causing a 1.9 °C rise in mean earth temperature and an increase of 3.8 meters in mean sea level.

With increasing attention on global warming internationally, many researchers have been focusing on effective ways to reduce carbon dioxide emissions to the atmosphere. This field has become to be known as carbon capture and storage (CCS). The capture of CO₂ from the flue gas of a power plant accounts three quarter the total cost of CCS. To achieve long range reduction rates of CO₂ emissions, cost effective CO₂ capture from fossil fuel power plant and subsequent sequestration options need to be industrialized. There are several

technologies available for CO₂ capture such as adsorption, absorption, membrane, gas separation, cryogenic separation, etc. CO₂ capture processes could be divided into three categories as follows:

- i. Precombustion – hydrocarbon fuels are decarbonized prior to combustion
- ii. Postcombustion – separation of CO₂ from the flue gases using different methods
- iii. Oxy-fuel combustion – the usage of pure oxygen separated from air

The three major CCS technologies listed above can be applied for power generation from coal (with the exception of some low rank coals due to unresolved engineering challenges) and natural gas. A recent study has analyzed the cost of electricity, efficiency and capital costs for three main capture technologies and concluded that oxy-fuel combustion has the largest potential for carbon capture and storage. Furthermore, capital cost analysis indicated that this technology is the most competitive option for retrofitting existing power plants. [3]

1.2. Oxy-fuel Combustion

During oxy-fuel combustion, fuel is burnt in a mixture of pure oxygen and recycled flue gas instead of air. The recycled flue gas in oxy-combustion aids in lowering the flame temperature and maintains a high gas volume through the reactor. The primary products of oxy-combustion are CO₂ and H₂O with a concentration of CO₂ ready for sequestration. This technology may provide a means whereby CO₂ can be more efficiently captured and other greenhouse gases such as NO_x can be minimized [4]. Oxy-fuel combustion is fundamentally different than conventional air combustion primarily due to the different physical and

chemical effects of CO₂ and H₂O. Recent reviews focused on solid fuels have discussed the challenges associated with this technology such as: commercialization at larger scales [5, 6], SO_x and NO_x emissions during solid fuel oxy-combustion [7] and the impacts of sulfur containing species [8], by summarizing the results from pilot and laboratory scale studies. From a technical perspective, a more complete understanding of flame ignition, stability and fuel burnout, heat transfer characteristics, formation of gaseous pollutants, ash and slagging propensities under oxy-fuel combustions have been identified as necessary to demonstrate this technology at larger scales.

1.2.1. Diffusion Oxy-methane Flames

The present study focuses on modeling laminar non-premixed combustion of methane under air-firing and oxy-firing conditions to validate recently developed chemistry and radiation property models. In non-premixed combustion, the fuel and oxidizer are fed separately into the furnace where the combustion takes place. Premixed combustion is another type of combustion in which the oxidizer and fuel mix before being fed into the combustion chamber. The non-premixed combustion is the prevalent mode of combustion in most industrial furnaces for safety concerns.

1.3. Numerical Modeling

High-Fidelity Computational Fluid Dynamic (CFD) simulations can provide valuable insights towards the design, operation and scale-up of oxy-combustion technologies. The CFD modeling approaches and sub-models employed in oxy-combustion are similar to those developed for conventional-air combustion. However, due to the high concentrations of CO₂ and H₂O with highly radiative properties, oxy-combustion is characterized by uncommon

heat transfer characteristics that are different from those encountered during air combustion cases. Recent reviews by Chen et al [9] and Edge et al [10] identified the need to refine and validate the models that were deemed to be accurate for fuel combustion with air and tailor them to work well under oxy-combustion scenarios. Among these, refining models for the gas-phase chemistry and gas-phase radiative properties have garnered much attention.

1.3.1. Radiative Heat Transfer

Unlike N_2 , a symmetric diatomic gas, CO_2 and H_2O absorb and emit radiation. During oxy-combustion, the high concentrations of CO_2 and H_2O may result in significantly different emissivities which in turn influence the absorption of heat within the boiler and enhances radiative heat transfer. Consequently, several existing models for computing total gas emissivity and absorptivity have been refined to accurately represent oxy-firing conditions. One of the most widely used models is the weighted sum of gray gases (WSGG) model which provides a good compromise between accuracy and computational resources. In this model, the total emissivity of a gas mixture is approximated as a weighted sum of a number of gray gases each with a distinct absorption coefficient. Therefore, a set of coefficients corresponding to each gas mixture is needed in order to be applied in the WSGG model. Recently, several models have been developed and validated. The WSGG model employed in this study uses the Statistical Narrow Band RADCAL database to determine the required emissivity data for fitting of the WSGG model. The model will be referred to as the Perry model and a more detailed description is found in [11].

1.3.2. Chemistry

Combustion occurs through a series of elementary chemical reactions which together

form a reaction mechanism. Detailed mechanism for the combustion of methane can include hundreds of chemical reactions which translate into a large set of differential equations to be solved in CFD simulations. Thus, several global mechanisms have been developed for the combustion of methane with a reduced set of reactions to model the reaction kinetics. The Westbrook-Dryer (WD) and Jones-Lindstedt (JL) are among the most used multi-step mechanism to model air combustion. These mechanisms were modified by Andersen et al to better model the reaction kinetics under oxy-firing conditions [12]. It has been shown that these models are able to give good predictions for temperature and major species such as CO_2 and H_2O , but fail to predict realistic and reliable predictions for CO. Chemistry models, such as the equilibrium model, that take into account intermediate combustion products resulted in better predictions. Thus, there is a need to better understand the limited capabilities of existing chemistry models. In order to carry out a rigorous assessment of chemistry models in oxy-combustion scenarios, experimental and numerical results from three, confined, laminar, diffusion methane flames are reported in chapter three of this thesis.

1.4. Thesis Outline

This thesis compiles a set of studies that investigates radiation and chemistry modeling strategies of oxy-methane combustion. In this chapter, the chemistry and radiation challenges encountered in modeling oxy-combustion are briefly presented. Chapter 2 examines gray and non-gray radiation modeling and their subsequent effect on variables important to radiative heat transfer by comparing model predictions to experimental measurements. In Chapter 3, the sensitivities of variables such as temperature and CO_2 predictions to the choice of chemistry model were studied. Chapter 4 investigates the

sensitivities of the radiative heat transfer to various radiation and chemistry models. Chapter 5 concludes the results obtained in this thesis.

1.5. References

- [1] Briefing, US Senate. "International Energy Outlook 2013." (2013).
- [2] IPCC. Policymaker's summary of the scientific assessment of climate change; report to IPCC from working group. Meteorological Office: Branknell, United Kingdom; 1990.
www.ipcc.ch/activity/srccs
- [3] J. Katzer, et al. "The future of coal: options for a carbon-constrained world." *Massachusetts Institute of Technology* (2007).
- [4] B.J.P. Buhre, L.K. Elliott, C.D. Sheng, R.P. Gupta, T.F. Wall, Oxy-fuel combustion technology for coal-fired power generation, *Progress in Energy and Combustion Science* 31 (2005) 283-307.
- [5] G. Scheffknecht, L. Al-Makhadmeh, U. Schnell, J. Maier, Oxy-fuel coal combustion a review of the current state-of-the-art, *International Journal of Greenhouse Gas Control* 5 (2011) S16-S35.
- [6] T. Wall, R. Stanger, S. Santos, Demonstrations of coal-fired oxy-fuel technology for carbon capture and storage and issues with commercial deployment, *International Journal of Greenhouse Gas Control*, *International Journal of Greenhouse Gas Control* 5S (2011) S5–S15.
- [7] M.B. Toftegaard, J. Brix, P. A. Jensen, P. Glarborg, A.D. Jensen, Oxy-fuel combustion of solid fuels, *Progress in Energy and Combustion Science* 36 (2010) 581-625.

- [8] R. Stanger, T. Wall, Sulphur impacts during pulverised coal combustion in oxy-fuel technology for carbon capture and storage, *Progress in Energy and Combustion Science* 37 (2011) 69-88.
- [9] L. Chen, S.Z. Yong, A.F. Ghoniem, Oxy-fuel combustion of pulverized coal: Characterization, fundamentals, stabilization and CFD modeling, *Progress in Energy and Combustion Science* 38 (2012) 156-214.
- [10] P. Edge, M. Gharebaghi, R. Irons, R. Porter, R.T.J. Porter, M. Pourkashanian, Combustion modelling opportunities and challenges for oxy-coal carbon capture technology, *Chemical Engineering Research and Design*, 89 (2011) 1470–1493
- [11] G. Krishnamoorthy, A new weighted-sum-of-gray-gases model for oxy-combustion scenarios, *International Journal of Energy Research* (2012) doi: 10.1002/er.2988
- [12] J. Andersen, C.L. Rasmussen, T. Giselsson, P. Glarborg, (2009). Global combustion mechanisms for use in CFD modeling under oxy-fuel conditions, *Energy & Fuels* 23 (2009) 1379-1389.

2. AN ASSESSMENT OF RADIATION MODELING STRATEGIES IN SIMULATIONS OF LAMINAR TO TRANSITIONAL, OXY-METHANE, DIFFUSION FLAMES

ABSTRACT

Twenty four, laboratory scale, laminar to transitional, diffusion oxy-methane flames were simulated employing different radiation modeling options and their predictions compared against experimental measurements of: temperature, flame length and radiant fraction. The models employed were: gray and non-gray formulations of a recently proposed weighted-sum-of-gray gas model, non-adiabatic extension of the equilibrium based mixture fraction model and investigations into the effects of: the thermal boundary conditions, soot and turbulence radiation interactions (TRI).

Predictions of gas, wall temperatures and flame lengths were in good agreement with experimental measurements. Flame lengths determined through the axial profiles of OH confirmed with the experimental trends by increasing with increase in fuel-inlet Reynolds numbers and decreasing with the increase in O₂ composition in oxidizer. The temperature and flame length predictions were not sensitive to the radiative property model employed.

There were significant variations between the gray and non-gray model radiant fraction predictions with the variations in general increasing with decrease in Reynolds numbers possibly attributed to shorter flames and steeper temperature gradients. The

inclusion of soot model and TRI model did not affect our predictions as a result of low soot volume fractions and the radiation emission enhancement to the temperature fluctuations being localized to the flame sheet.

2.1. Introduction

2.1.1. Numerical Modeling of oxy-fuel combustion

Modified radiative property models in the form of weighted-sum-of-gray-gases (WSGG) coefficients [1-4] and modified global kinetic mechanisms [2, 5-7] for oxy-combustion scenarios have been proposed. WSGG models are popular due to: their ease of implementation within CFD frameworks, computational cost and accuracies, and the ability to employ them in their gray or non-gray formulations. In previous studies [1-4], the accuracies of the proposed WSGG models were first assessed by comparisons against benchmark solutions in prototypical geometries with media conditions representative of oxy-combustion. They were then subsequently employed in CFD calculations where the radiation models were coupled to other combustion models. The main conclusions from these studies are summarized here.

- Although different spectroscopic databases were employed in the formulation of WSGG models, the EM2C statistical narrow band (SNB) and RADCAL SNB model databases were deemed as most accurate for WSGG model formulations [1]. Recently, a WSGG model has also been proposed by directly employing the HITEMP 2010 database [4].
- Through oxy-combustion simulations of natural gas in large scale furnaces Yin [9] and Krishnamoorthy [1] concluded that non-gray radiative transfer models are more important for an accurate determination of wall fluxes rather than temperatures but

- acknowledged that the presence of particles (that can be approximated as gray radiators to a good approximation) can minimize the importance of non-gray gas radiation models.
- In a subsequent study by Nakod et al [10], simulations of oxy-coal combustion revealed that in small scale furnaces where the particle radiation is greater than the gas radiation, the differences between gray and non-gray radiation modeling strategies were minimal. However, in full-scale boilers the wall radiative flux predictions were significantly different between the gray and non-gray models due to large volume pockets within the furnace where the gas radiation dominated over the particle radiation. Kangwanpongpan et al [11] through numerical investigations on a swirling oxy-coal flame in a lab-scale furnace attributed an improved agreement between the numerical temperature predictions with the experimental data to the use of a non-gray model.
 - Through simulations of oxy-propane flames in a lab-scale furnace, Hjartstam et al [6] concluded that while non-gray radiation had an impact on the radiation field and temperature, accurate soot models are more important than the non-gray models.
 - Due to the large concentrations of radiatively participating gases during oxy-combustion, accurately accounting for turbulence radiation interactions (TRI) has been determined to be important [12]. Accurately accounting for TRI in oxy-combustion simulations was determined to be important in oxy-coal combustion studies [13] and natural gas combustion experiments [14]. However, a numerical investigation of highly swirling natural-gas flame showed that TRI does not play a significant role in oxy-combustion [1].

2.1.2. Motivation for the Present Study

As seen from the summary of previous studies, due to differences in fuel type (in terms of the sooting propensities for the gaseous fuels and coal type employed in the solid fuels), configuration and size of the furnaces, there is still considerable uncertainty in the a priori identification of oxidizer compositions to be employed during oxy-combustion that will result in temperature and radiative heat flux profiles that are similar to those encountered during combustion in air. Due to the difficulties in obtaining radiative flux measurements in large scale boilers, it is therefore pivotal that the radiation and combustion modeling procedures achieve a high degree of fidelity. However, there is some disagreement on the relative importance of non-gray radiation modeling and TRI modeling in oxy-combustion scenarios and their subsequent impact on the temperature and radiative heat fluxes. A quantification of their individual effects and associated uncertainties are made difficult due to the presence of particles (soot or coal) and associated uncertainties with the turbulence and chemistry models. Therefore, the goal of this study is to carry out an assessment and validation of gray and non-gray models in oxy-combustion scenarios by comparing model predictions against experimental measurements of variables important to radiative transfer in well-controlled laminar to transitional, oxy-methane, diffusion flames. By restricting ourselves to laminar to transitional flow conditions and a mildly sooting fuel, we attempt to minimize the impact of the turbulence modeling procedure and the uncertainties associated with the particle contribution to radiation.

2.2. Laminar to Transitional, Oxy-Methane, Diffusion Flames

The oxy-flames simulated in this work were experimentally investigated by Ditaranto and Oppelt [15]. They present experimental results of radiative heat flux along the axial

direction, flame lengths and radiant fractions of twenty-four non-premixed jet methane flames developing in oxy-fuel environments. Six different oxidizer compositions with oxygen concentrations ranging from 35% to 70% with CO₂ as the diluent, as well as in air were considered along with four fuel inlet Reynolds numbers ranging from 468 to 2340. Therefore, their experiments represent a nice dataset for the validation of radiation models for a wide range of O₂-CO₂ compositions in the oxidizer stream, at laminar to transitional conditions with minimal interference of particle radiation (soot). All 24 flames investigated by Ditaranto and Oppelt [15] were simulated in this study employing different modeling options.

2.3. CFD Modeling Approach

2.3.1. Geometry and Mesh

The furnace consists of a fuel nozzle of diameter 5 mm, oxidizer nozzle of diameter 100 mm enclosed in a combustion chamber of diameter 350 mm and 1000 mm in length with stainless steel walls. The co-flow velocity of the oxidizer stream was maintained at 0.25 m/s with the fuel jet velocities varying between 1.5 m/s and 7.6 m/s to represent four Reynolds numbers in the range 468 and 2340 [15]. The inlet temperatures of the fuel and oxidizer were set at 288 K for the fuel densities to match the fuel inlet Reynolds numbers at the different jet velocities [16].

The CFD simulations were carried out using the commercial code ANSYS FLUENT [17]. The furnace was modeled in a 2D axisymmetric domain to take advantage of the symmetry of the problem. The entire geometry was meshed employing 30,700 hexahedral control volumes. Simulations were also repeated employing 263,000 control volumes and the

results of the variables reported in this study were found to be identical at both these mesh resolutions. All the flames investigated in this study were determined to be in the buoyant regime since their laminar Froude numbers were less than unity [15]. The pressure velocity coupling was therefore accomplished using the SIMPLEC algorithm which we have determined from past experience to perform well in such buoyancy driven enclosure flows. The PRESTO and QUICK schemes were employed for the spatial discretization of the pressure and momentum terms respectively since hexahedral cells were employed in the calculations [17]. The buoyancy within the domain necessitated performing transient simulations. Although, a time step size of 0.001 seconds was employed in all the calculations, all of the reported variables in this study converged to a constant value. The turbulence was modeled using the standard k- ϵ turbulence model [17].

2.3.2. Radiation Modeling and Boundary Conditions

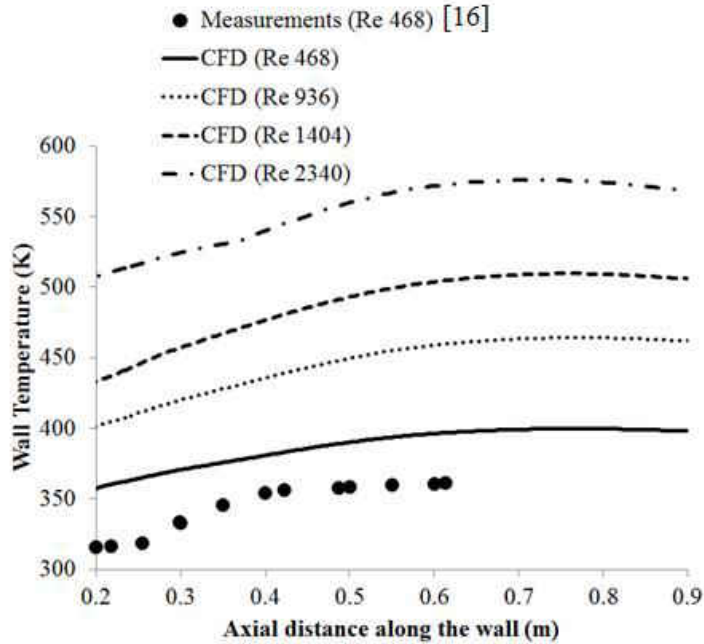
The radiation was modeled by solving the radiative transport equation (RTE) employing the Discrete Ordinate (DO) model. The angular discretization was carried out by employing a 4 x 4 theta x phi discretization. The adequacy of this angular resolution was established by determining that the reported variables did not change with any further increase in angular resolution.

To determine the radiative property of the gas mixture, a recently proposed WSGG model [1] that is based on the SNB RADCAL database was implemented as a user-defined function (UDF) and employed in the combustion simulations. The WSGG model accurately calculates the radiative properties of CO₂ and H₂O vapor mixtures that are encountered in scenarios encompassing methane, natural gas or coal combustion under air-fired and oxy-

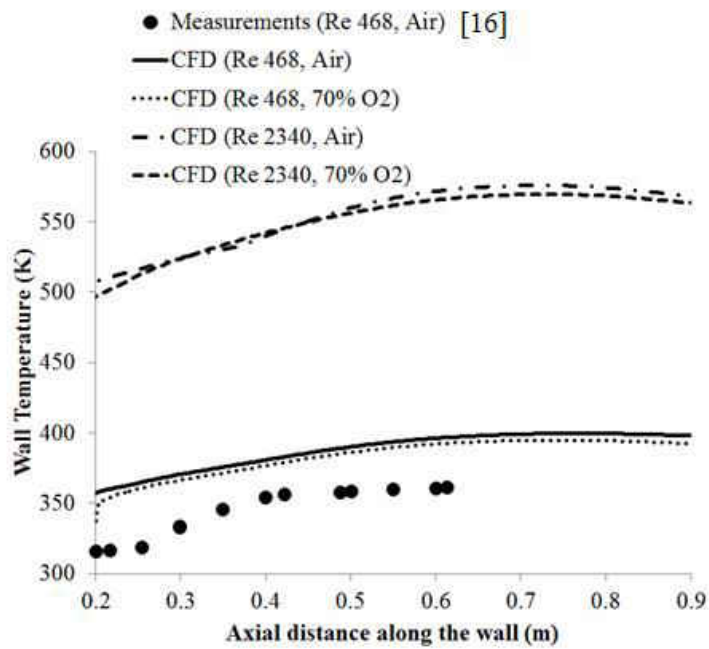
fired conditions. Both gray and non-gray formulations (with five gray gases) of the WSGGM were employed in this study. We have previously demonstrated that radiative transfer predictions employing the non-gray model when employed in conjunction with the discrete ordinates (DO) method, compares well against line-by-line (LBL) benchmark data based on the latest spectroscopic database (HITEMP 2010) that have been made available recently [1, 18]. The comparisons against the LBL benchmark data were carried out for a prototypical problem that was representative of a laminar, oxy-methane diffusion flame with dry flue gas recycle which is similar to the flames investigated in this study. The model was also shown compare well against the EM2C SNB model calculations that have served as benchmark data in three-dimensional geometries.

For the radiation boundary conditions, the stainless steel walls of the reactor were assigned an emissivity of 0.98 at the inside walls of the reactor [15]. The external walls (assigned an emissivity of 0.7) were assumed to radiate to the ambient air at 300 K and the reactor wall temperature was established by an energy balance between the net radiative and convective heat fluxes at the inside walls of the reactor and the net emission from the outside wall of the reactor. The non-availability of the steady-state wall temperature profiles for all the flames necessitated the adopting of a physically realistic thermal boundary condition. Figure 2-1 compares the steady state axial wall temperature profile that evolved as a result of the above imposed radiative boundary conditions for the different flames compared against wall temperature measurements of the methane-air flame at Re 468 obtained from Ditaranto et al [16]. First, the observed agreement between the numerical predictions and experimental measurements is within 50K. Second, from Figure 2-1a the wall temperatures are seen to depend on the fuel inlet Reynolds numbers. Higher Reynolds numbers result in larger flame

lengths and flame volumes thereby resulting in higher wall temperature profiles. Figure 2-1b compares the effect of oxidizer compositions (air and 70% O₂-30% CO₂) on the evolved wall temperature profiles at the lowest and highest fuel inlet Reynolds numbers investigated in this study. Although higher O₂ concentrations result in higher flame temperatures, the flame lengths decrease with increase in oxidizer compositions [15]. Therefore, at higher O₂ concentrations, the net effect of increase in radiation due to higher flame temperature is offset by a decrease in radiation due to a reduction in flame volume, thereby resulting in a wall temperature profile identical to that obtained during methane-air combustion.



(a)



(b)

Figure 2-1: Temperature profiles predicted along the height of the wall for: (a) Methane-Air flames at different fuel inlet Reynolds numbers; (b) Methane-Air flames and oxy-methane flames at fuel inlet Reynolds numbers of 468 and 2340.

2.3.3. Chemistry Modeling

The effects of high CO₂ concentration encountered during oxy-combustion on the methane combustion chemistry have been extensively studied [19, 20]. Glarborg and Bentzen [19] proposed that oxy-fuel combustion will lead to strongly increased CO concentrations in the near-burner region with the CO₂ in the oxidizer stream competing with O₂ for the atomic hydrogen through the equilibrium reaction: $\text{CO}_2 + \text{H} \leftrightarrow \text{CO} + \text{OH}$ and resulting in the formation of more CO. Amato et al. [20] concluded that this CO₂ destruction reaction along with the destruction of O₂ through the reaction $\text{O}_2 + \text{H} \leftrightarrow \text{O} + \text{OH}$ were the key reactions controlling the concentrations of CO₂ and O₂ in the post-flame zone. From a radiative heat transfer perspective, these key reactions not only determine the concentrations of the radiatively participating gases CO and CO₂ but also alter the concentrations of the O/H/OH radical pool which determine the rate of soot oxidation [21]. Furthermore, the numerical predictions of the OH concentrations provide us with an estimate of the flame length to enable comparisons against experimentally determined flame lengths. Due to the computational cost associated with the use of detailed chemical mechanisms in CFD simulations that enable an accurate prediction of these radicals, most of the previous numerical investigations of oxy-methane diffusion flames have employed global reaction mechanisms with rate parameters modified to oxy-combustion conditions [5, 22, 23]. While global reaction mechanisms gave reasonable predictions of CO₂, H₂O and temperature they failed to predict the CO concentrations accurately [23].

In this study, the non-adiabatic extension of the equilibrium PDF model was employed in the calculations for modeling the chemistry. Here, the instantaneous thermochemical state of a fluid is related to its mixture fraction and its enthalpy. The benefits

of this model is that by assuming equal species diffusivities, the individual species conservation equations reduce to a single “sourceless” conservation equation for the mixture fraction as a result of the cancellation of the reaction source terms in the species equations due to elemental conservation. This enables us to estimate the concentrations of minor species such as OH as well as get accurate predictions of the flame temperature (which is pivotal to estimating the radiant fractions) in a computationally efficient manner without the need to resort to a detailed chemical mechanism that is applicable to oxy-combustion conditions.

Under the assumption of chemical equilibrium, all thermochemical scalars (species fractions, density, and temperature) are uniquely related to the mixture fraction(s) and the value of each mass fraction, density and temperature were determined from calculated values of mixture fraction, variance in mixture fraction and the enthalpy. Twenty chemical species were considered in the equilibrium calculations (CH_4 , C_2H_2 , CH_3 , C_2N_2 , C_2H_6 , C_2H_4 , C_4H_2 , C_3H_3 , HNC , $\text{C}(\text{s})$, CO , CO_2 , H_2O , OH , N_2 , O_2 , H , O , HO_2 and H_2). An assumed shape probability distribution function (PDF) was employed to describe turbulence-chemistry interactions where the average value of the scalars is related to their instantaneously fluctuating values. In this study, the shape of the PDF was described by the beta function.

2.4. Results and Discussion

2.4.1. Temperature and Flame Lengths

Figure 2-2 shows the temperature contours (in K) within the reactor at different oxidizer compositions and at various Reynolds numbers. Although the calculations were performed with both the gray and non-gray formulations of the WSGG model proposed by Krishnamoorthy [1], the temperature contours in Figure 2-2 correspond to the results from

the non-gray model. As expected and confirmed by experimental observations [16], the flame length increases with increase in Reynolds number and the peak flame temperature increases with an increase in O₂ concentration in the oxidizer. Marked temperature gradients are observed in the lower section of the furnace away from the flame particularly at higher Reynolds numbers. This is indicative of buoyancy induced natural convection patterns within the furnace. However, since the equilibrium PDF model assumes equal species diffusivities and neglects Soret diffusion, a preliminary investigation of the importance of Soret diffusion was carried out employing a 41-step reduced CH₄-Air kinetic mechanism. The flame length and radiant fraction predictions from employing the 41-step mechanism did not change as a result of including Soret diffusion even in the 70% O₂ flame where the highest temperatures were encountered.

In this study, to determine the radiant fractions from these flames, the incident radiative fluxes along the furnace walls were integrated. Due to these strong buoyant flows, the wall integrated incident radiative fluxes did not converge to a constant value in these larger Reynolds number flames when employed in a steady state calculation. Therefore, we had to perform these calculations employing an unsteady solver as indicated previously to obtain a constant value for the wall integrated incident radiative fluxes.

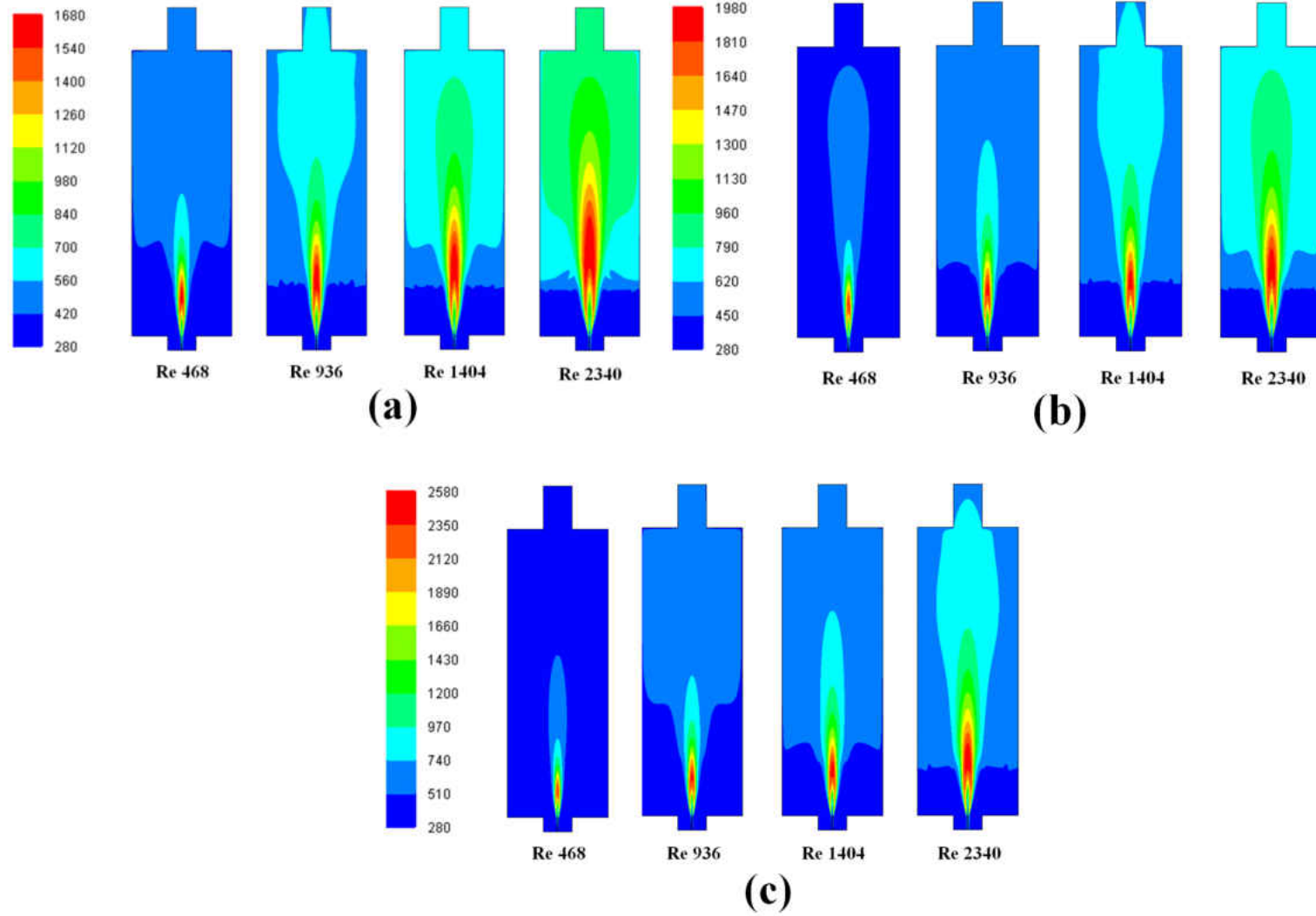


Figure 2-2: Temperature contours (in K) within the reactor at different oxidizer compositions: a) air, b) 40% O₂ in CO₂, c) 70% O₂ in CO₂.

Figure 2-3 compares the radial temperature profile predictions at different axial locations within the reactor for the oxy-methane flame (Re 1404; 35% O₂ - 65% CO₂ oxidizer composition) against experimental measurements from Mario et al. [16]. CFD predictions are with the non-gray WSGGM. The observed agreement between the numerical predictions and experimental observations is good, confirming the adequacy of our modeling approach.

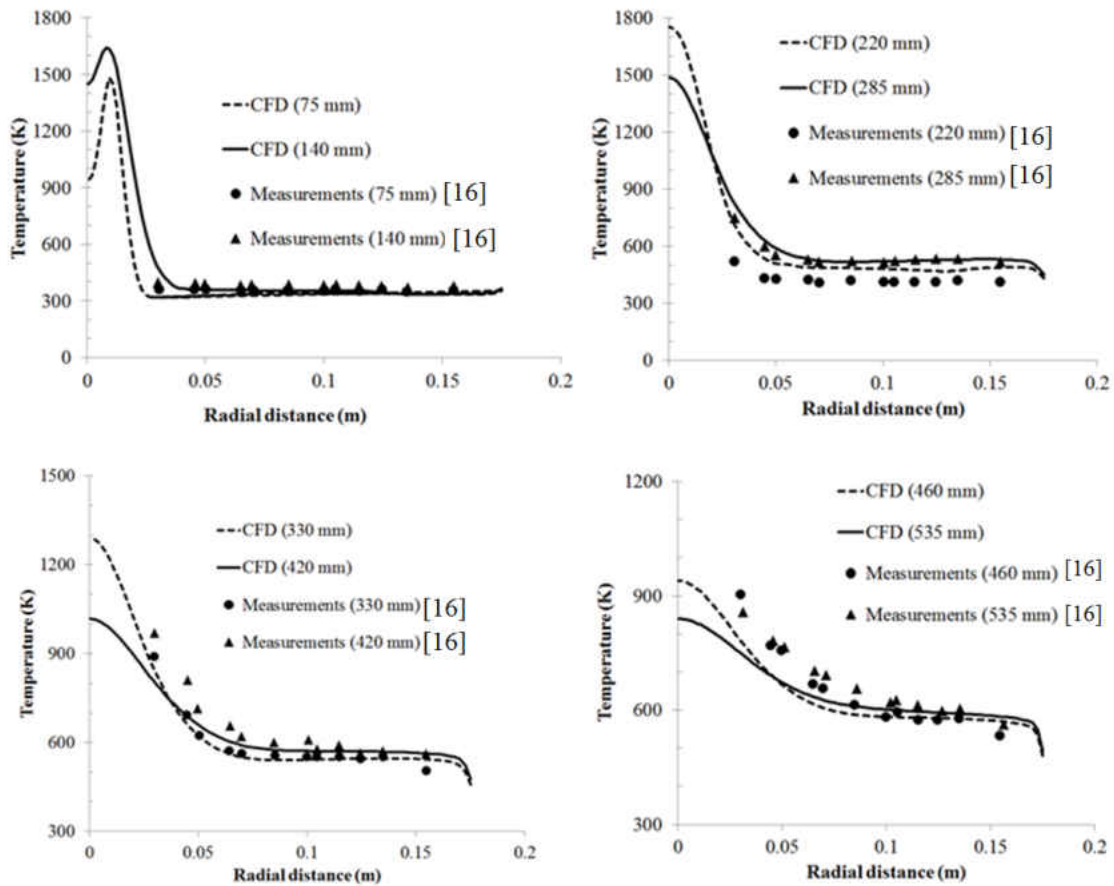


Figure 2-3: Radial temperature profiles at different axial locations within the reactor for the Oxy-methane flame (Re 1404; 35% O₂ - 65% CO₂ oxidizer composition). CFD predictions are with the non-gray WSGGM.

Figure 2-4 compares the radial temperature predictions between the gray and non-gray WSGGM calculations in this flame. A soot model was not employed in these

calculations. From Figure 2-4 it can be inferred that the differences in gas temperature predictions between the gray and non-gray models are minimal at these oxidizer compositions in oxy-methane flames.

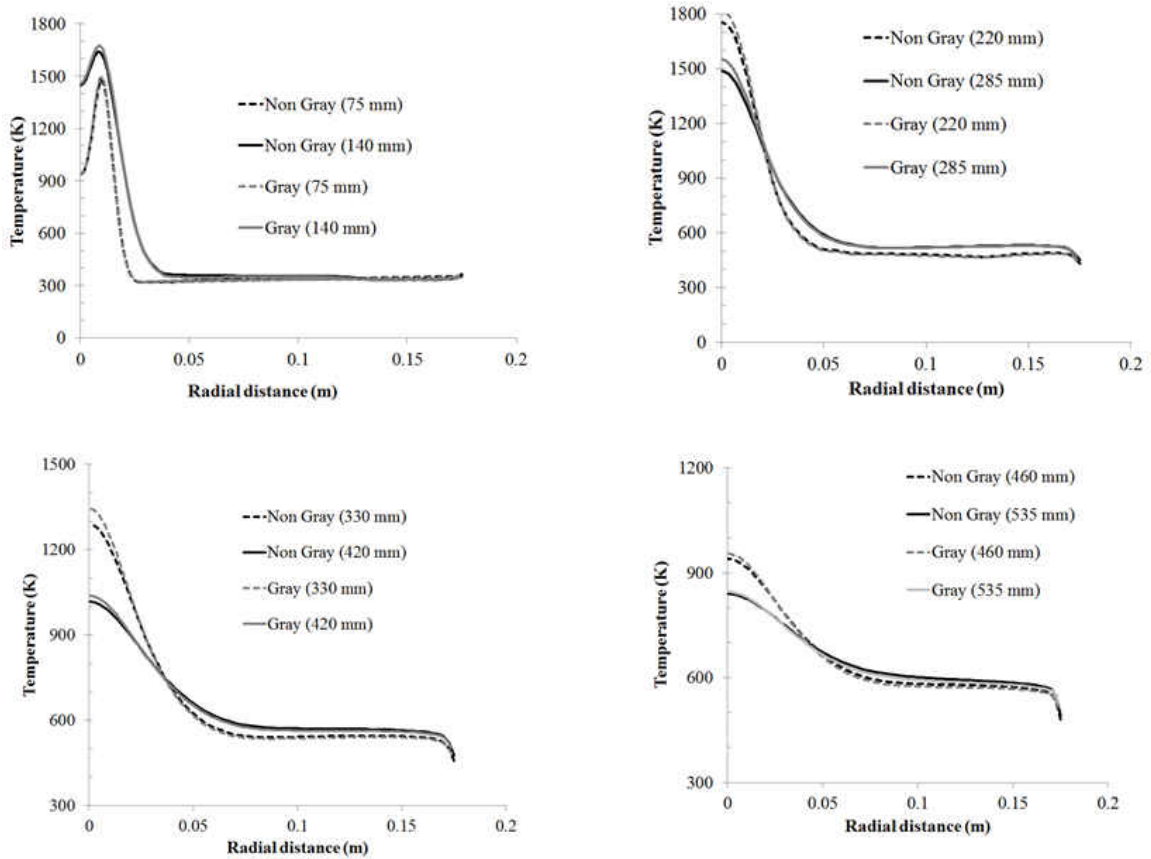


Figure 2-4: Radial temperature profiles at different axial locations within the reactor for the oxy-methane flame (Re 1404; 35% O₂ - 65% CO₂ oxidizer composition).

Since flame lengths are determined experimentally by OH radical emissions [24], the flame centerline OH concentration profiles were employed in this study to estimate the flame lengths numerically. Figure 2-5 compares the predicted flame lengths employing gray and non-gray models against experimental measurements for the different oxidizer composition streams and Reynolds numbers investigated in this study. First, very good agreement is observed between numerical predictions and experimental measurements with the agreement in general improving at higher Reynolds numbers.

Second, the differences in flame length predictions between the gray and non-gray radiation models are minimal. The percentage variation between the numerical predictions of flame length employing the non-gray model and the experimental observations are summarized in Table 2-1. While the experimental data show a linear trend in flame length predictions as a function of the O₂ concentrations in the oxidizer stream, the deviations from the linear trend in our numerical predictions at 70% O₂ concentration are likely due to the approximations inherent in the equilibrium PDF model, namely that of equal species diffusivities. While this shortcoming is likely to become less important with increase in Reynolds numbers, full multi-component diffusion coefficients need to be employed in conjunction with a detailed chemistry mechanism at diffusion-dominated laminar flow conditions. The improvement in the results at higher Reynolds numbers demonstrate that the non-adiabatic extension of the equilibrium PDF chemistry model in conjunction with the gray/non-gray formulation of our recently proposed WSGGM may be successfully employed to predict the flame lengths during oxy-combustion in larger scale reactors. The decrease in flame length with the increase in O₂ composition in the oxidizer stream may be attributed to the increased temperature and radical diffusion encountered under those conditions. The increase in stoichiometric mixture fraction at higher O₂ compositions also alters the flame shape by displacing the flame front closer to the centerline, where a lower degree of mixing has been achieved [15].

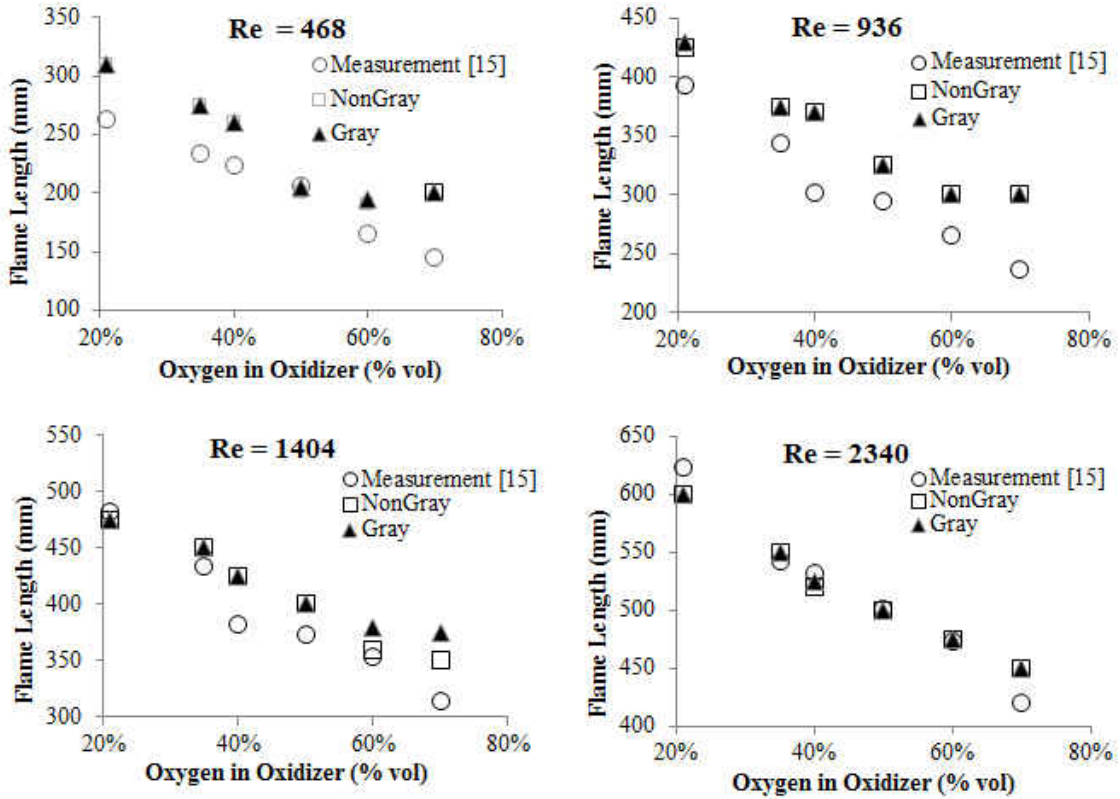


Figure 2-5: Flame length predictions employing gray and non-gray models as a function of oxygen compositions in the oxidizer and fuel inlet Reynolds numbers.

Table 2-1: Percent variation between the numerical predictions of the flame length and the experimental values for the gray and non-gray models.

O ₂ (% vol)	Gray (% error)				Non-Gray (% error)			
	Re 468	Re 936	Re 1404	Re 2340	Re 468	Re 936	Re 1404	Re 2340
21	18	9	1	4	18	8	1	4
35	18	9	4	1	18	9	4	1
40	16	23	11	2	16	23	11	2
50	0	11	7	0	3	11	7	0
60	17	13	8	0	14	13	2	0
70	38	27	19	7	38	27	11	7

Figure 2-6 shows the predicted axial OH profiles for three different oxidizer compositions at Reynolds numbers of 468 and 2340. The OH concentrations are very sensitive to the oxygen concentrations in the oxidizer increasing significantly with an

increase in O_2 concentration in the oxidizer. This trend which has been observed experimentally as well [15, 25], may be attributed to the increase in temperature and the availability of more oxygen atoms in the flames with the oxygen-enriched oxidizer.

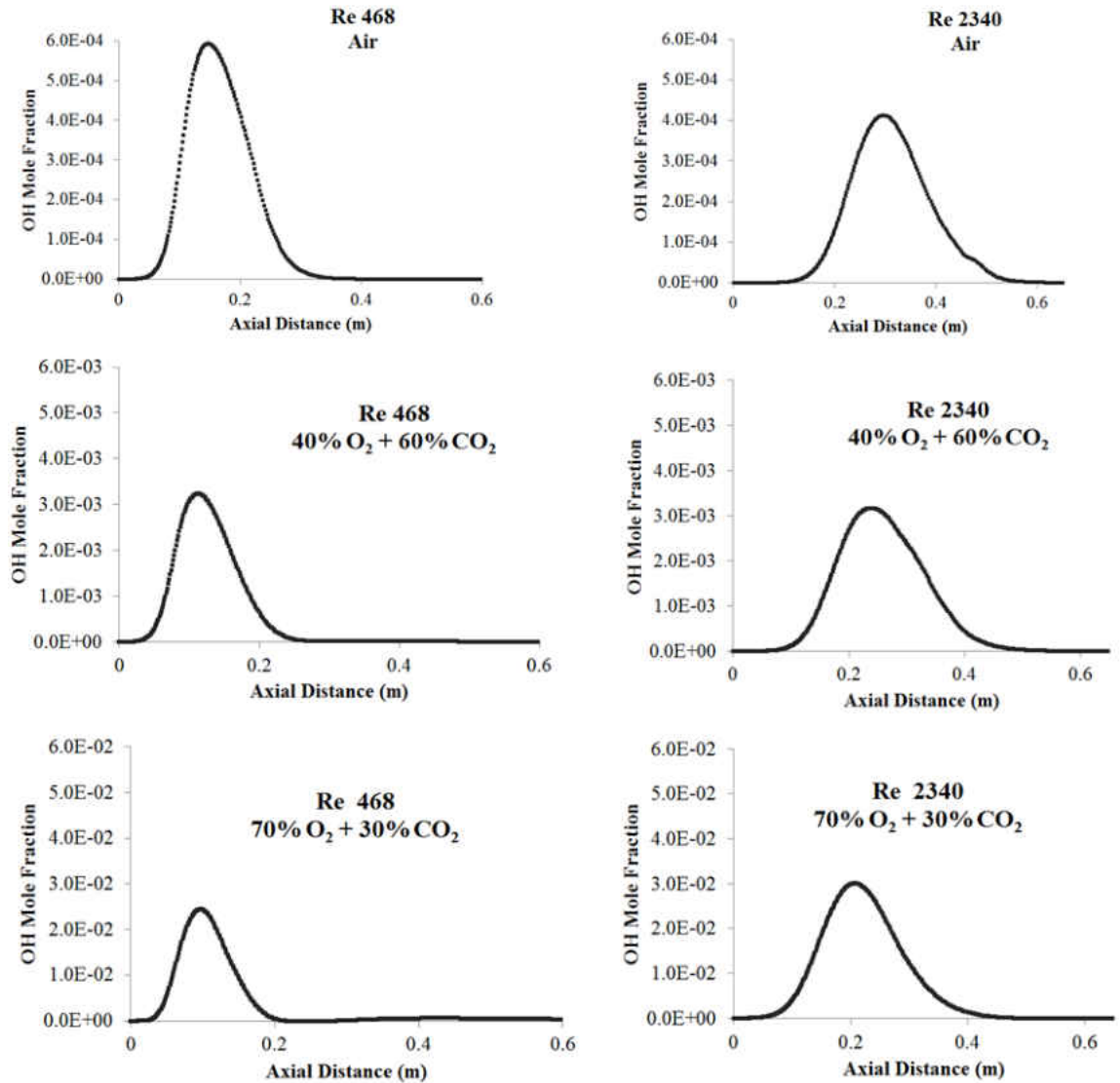
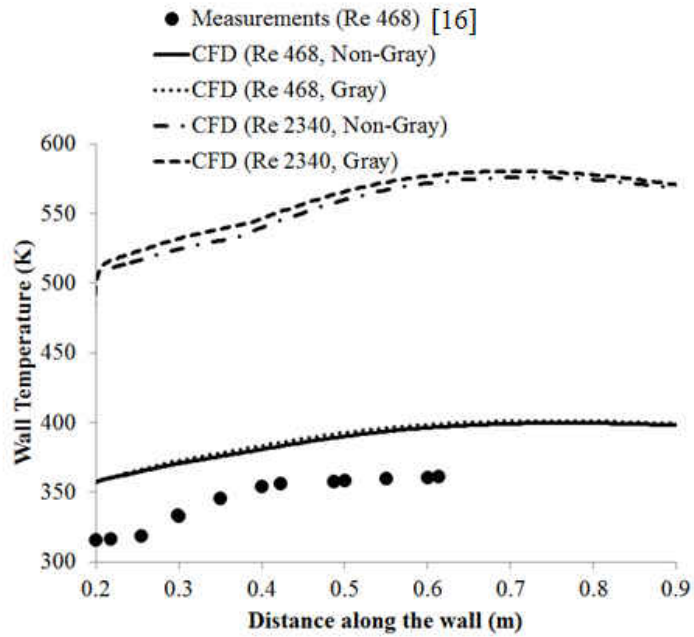


Figure 2-6: Predictions of the axial variations in the OH mole fractions in different flames.

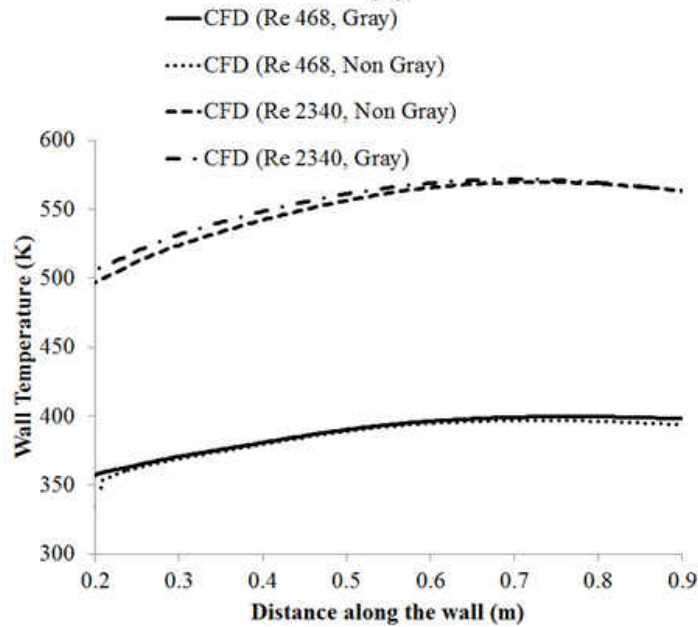
2.4.2. Radiant Fraction Predictions

Figure 2-7 compares the temperature profiles predicted along the height of the wall employing gray and non-gray radiation models for the methane-air flames and oxy-methane

flames (70% O₂). The wall temperatures like the gas temperatures (cf. Figure 2-4) are not sensitive to the gas radiative property model employed in the calculations.



(a)



(b)

Figure 2-7: Temperature profiles predicted along the height of the wall employing gray and non-gray radiation models for: (a) Methane-Air flames; (b) Oxy-methane flames (70% O₂).

Figure 2-8 compares the numerical predictions of the radiant fraction in the flames at various oxidizer compositions and Reynolds numbers. The radiant fraction was numerically estimated as the surface integral of the incident radiative flux along the side walls divided by the total thermal input of the various flames. The thermal input of the flames was computed as the product of the low heating value of methane and its mass flow rate. Although, the experimental measurements of the radiant fraction from Ditaranto and Oppelt [15] are also shown in Figure 2-8, there are significant differences between the method that was employed to estimate the radiant fraction experimentally and the numerical estimation adopted in this study. Ditaranto and Oppelt [15] estimated the incident radiative heat flux measured by the sensor by establishing a radiative energy balance at the sensor surface. By taking measurements of the wall and gas temperatures and the gas composition profiles (CO, CO₂ and H₂O) around the flames at different heights, the radiant intensity incident on the sensor surface from the non-homogenous, non-isothermal gas volume along the line-of-sight of the sensor was estimated employing the SNB RADCAL. Next, the radiant intensities were integrated over a hemisphere and multiplied by configuration factors calculated using a Monte Carlo ray tracing method adapted to their reactor configuration. Therefore, a major difference in the methodologies for estimating the radiant fraction between the two studies stems from the fact that experimentally, a global gray-gas absorption coefficient (α_g in [15]) estimated from the SNB RADCAL was employed to compute the incident radiation on the sensor by solving the RTE in one-dimension, whereas in this study the RTE is being solved in two-dimensional axisymmetric co-ordinate system with the gray and non-gray gas absorption coefficients computed based on our recently proposed WSGGM. Second, although the WSGGM is also based on the SNB RADCAL model, the computed gray gas

absorption coefficients in the experimental study and this study could be significantly different due to the differences in the radiation path-length or mean beam lengths employed in the calculation to estimate the gas absorption coefficients from the total emissivities. In one-dimensional RTE calculations, the path-length corresponds to the length of the radiant ray whereas in our study the path-length corresponds to the geometric mean beam length of the reactor geometry which is a function of the reactor volume and surface area. Finally, wall temperature measurements were employed by Ditaranto and Oppelt [15] to correct for the background radiation in the 1D radiation calculations. Differences between the measured instantaneous wall temperatures and the numerically estimated steady state, wall temperature for the various flames [cf. Figure 2-1 and Figure 2-7] could be an additional contributing factor to the observed differences between the numerical prediction and experimental observations in Figure 2-8. However, the experimentally observed trends of increase in radiant fraction with increase in Reynolds numbers and the increase in oxygen concentrations in the oxidizer are also predicted numerically. It is also evident from Figure 2-8 that the non-gray model predicts lower radiant fraction (as a result of lower incident radiative flux predictions) than the gray model. Similar observations between the gray and non-gray model predictions were reported by Yin [9] in simulations of oxy-combustion of natural gas in large scale furnaces and by Nakod et al [10] in their simulations of oxy-coal combustion in large scale furnaces.

Table 2-2 displays the percentage deviation of the gray model estimates of the radiant fraction from the corresponding non-gray radiant fraction estimates. At a given oxidizer composition, the variations between the gray and non-gray model predictions increases with decrease in Reynolds numbers. This is attributed to the fact that sharper temperature gradients (as a result of smaller flame lengths) are encountered in the lower Reynolds number flames while the peak temperatures and the average medium compositions remain approximately the same at a given oxidizer composition. Since gray models are based on fits to the total-emissivity data, they are very accurate in estimating the total gas emissivities and therefore the radiative heat fluxes in homogeneous, isothermal media. However, as the non-homogeneities and temperature gradients increase, the gray models are found to be less accurate [26].

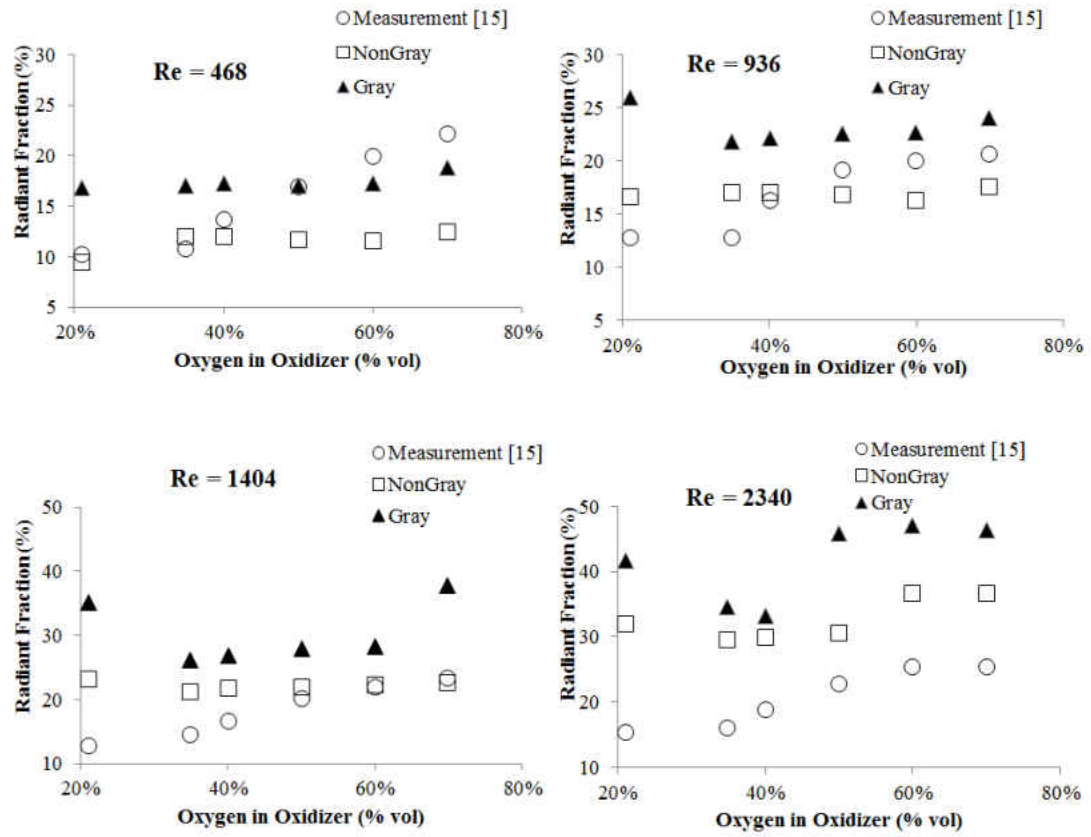


Figure 2-8: Radiant fraction loss predictions employing gray and non-gray models at various oxidizer compositions and Reynolds numbers.

Table 2-2: Percentage deviation of the gray model estimates of the radiant fraction from the corresponding non-gray radiant fraction estimates.

O ₂ (% vol)	Gray/Non-gray % variation			
	Re 468	Re 936	Re 1404	Re 2340
21	77	57	53	30
35	42	29	23	17
40	44	30	24	11
50	46	34	26	50
60	49	39	29	28
70	51	37	68	26

2.4.3. Effects of Soot Model

As observed in Figure 2-8, at a given Reynolds number, the radiant fraction increases with an increase in oxygen concentration in the oxidizer. The flame temperature increases with the increase in oxygen composition in the oxidizer but the flame length decreases. Ditaranto and Oppelt [15] attributed this to an increase in the soot inception rates at higher oxygen concentrations that results in higher soot concentrations and therefore higher soot emissions in the oxygen-rich flames. While our simulations in Figure 2-8 that were carried out without any soot models were able to qualitatively capture the observed experimental trends in radiant fraction, the effect of including soot in the calculations was investigated next. The implementation of the Moss-Brooks soot model [27] in ANSYS FLUENT that has mainly been developed and validated for methane flames was employed to predict the soot volume fractions in the different flames. Figure 2-9 compares the axial soot volume fraction predictions employing the non-gray model at Reynolds number 468 and 2340 for several oxidizer compositions. Contrary to the deductions of Ditaranto and Oppelt [15], the soot volume fraction decreases with higher oxygen in the oxidizer possibly due to the increased

oxidation of soot by the OH radicals [cf. Figure 2-6]. Soot formation rates however have been observed to increase with increase in Reynolds numbers due to shorter residence times and incomplete mixing.

Figure 2-10 shows the effect of including the soot participation in the radiant fraction calculations performed employing the non-gray WSGGM. As a result of the low soot volume fractions predicted in the simulations, the presence of soot is observed to have a negligible effect on the radiant fraction predictions.

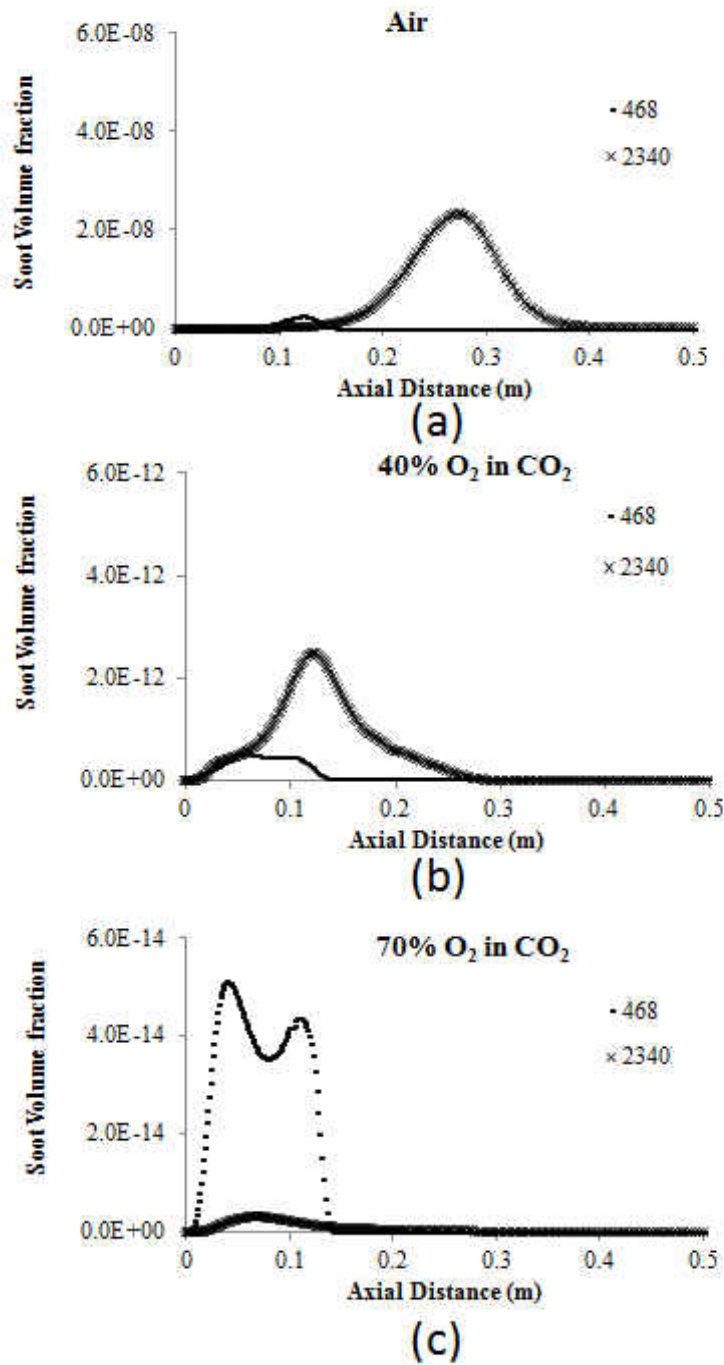


Figure 2-9: Soot volume fraction predictions employing the non-gray model at Reynolds number 468 and 2340 for several oxidizer compositions.

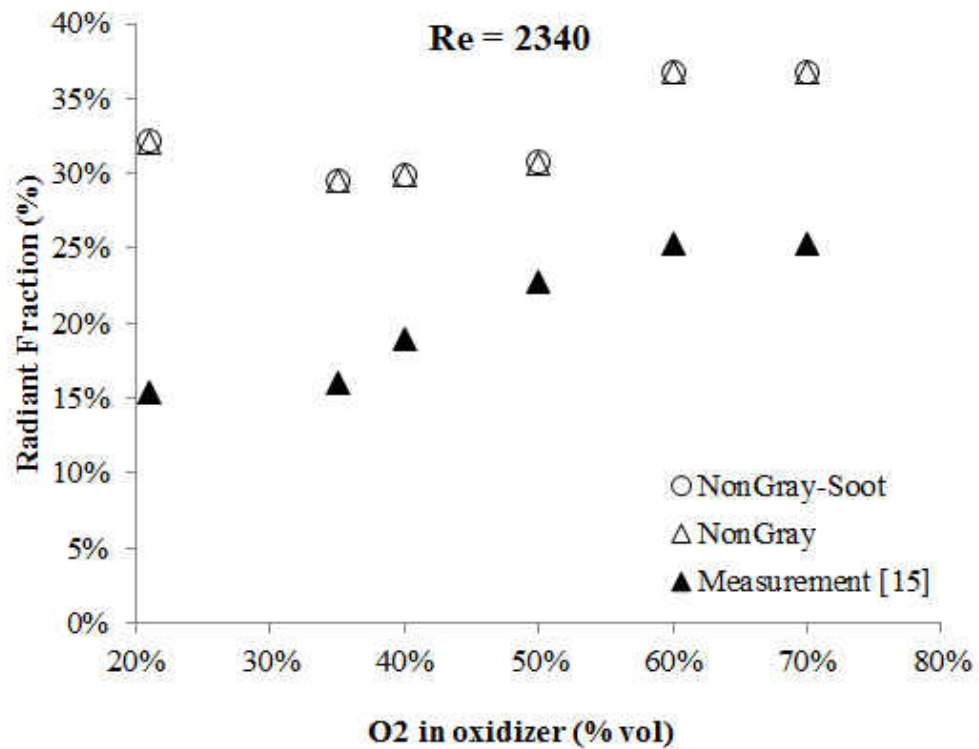
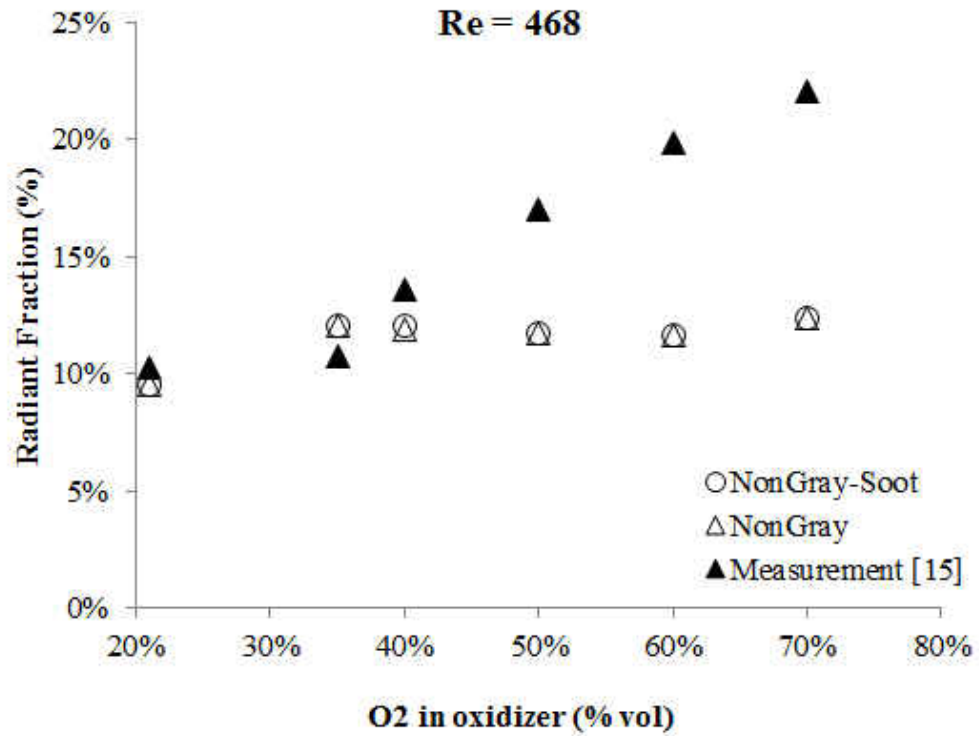


Figure 2-10: Effect of soot on the radiant fraction at Re 468 and Re 2340.

2.4.4. Turbulence Radiation Interaction (TRI) Model

It is well known that accounting for TRI could result in an enhancement in the radiative fluxes in diffusion flames. This has been attributed more due to the temperature fluctuations in the emission term rather than the fluctuations in the absorption coefficients in both optically thin as well as optically thick systems [28, 29]. The current state of the art in modeling TRI has been reviewed by Coelho [30]. TRI effects are generally accounted for using the time-averaged radiative transport equation (RTE) or the Monte Carlo method that rely on the optically thin fluctuation approximation by neglecting the correlation between fluctuations of the absorption coefficient and the fluctuations of the radiation intensity. In this study, a preliminary investigation of TRI is carried out by assuming that the effects of TRI are dominated by the fluctuations in the temperature or the temperature self-correlation term. The essence of computing the temperature self-correlation in TRI models reduces to the calculation of $\overline{T^4}$ in the emissive power term in the time-averaged RTE. Burns [31] showed that $\overline{T^4}$ can be approximated from mean and standard deviation (root-mean-square, rms) of temperature by expanding the Planck's black body emissive power in a Taylor series about the mean temperature and time averaging. Accordingly, the mean temperature and T_{rms} fields were then employed to obtain time-averaged black body emissive power according to the relation:

$$\frac{\overline{T^4}}{\overline{T}^4} \approx \left\{ 1 + 7.5 \frac{\overline{T'^2}}{\overline{T}^2} \right\} \quad \text{Equation 2-1}$$

In this study, preliminary investigations of TRI were carried out in the methane flames by modifying the emissive power term in the RTE according to Equation 2-1 through a user-defined-function in ANSYS FLUENT version 12. This was done to ascertain that TRI

modeling does not significantly affect the fidelity of our calculations. Figure 2-10 shows the emission enhancement in different flames (the left hand side of Eq. 1) that arise as a result of temperature fluctuations due to turbulence. It is worth noting that the emission enhancement in these flames is localized to the flame sheet. However, they can be significant at the flame sheet where an enhancement of up to 2.5 times is observed. However, due to the localized enhancement, the radiative fluxes at the walls (and consequently the radiant fractions) did not change as a result of including the TRI model. However, in more turbulent systems where the temperature fluctuations are more prevalent, the TRI models may affect the wall radiative fluxes [1]. Furthermore, the localized emission enhancement in these flames may play an impact in determining the local flame temperatures and consequently the formation of soot, NO_x and flame extinction in more strongly radiating systems.

As a result of the low Froude numbers, the investigated flames are buoyancy dominated, resulting in fluctuations in the flow and temperature fields. To investigate if the low frequency fluctuations that are not captured in a RANS simulation employing the 2D axisymmetric assumption have an impact on our predictions, 3D Large Eddy Simulations (LES) employing 1.7 million computational cells of the flame at Re 1404 and 21% O₂ oxidizer concentration were carried out. The calculations resulted in the same flame length as that of the 2D RANS calculation reported in this study. Furthermore, the LES calculations in conjunction with the contours of emission enhancement shown in Figure 2-11 confirmed that the importance of TRI resulting from these fluctuations and its subsequent impact on the radiant fraction predictions was not significant in these flames.

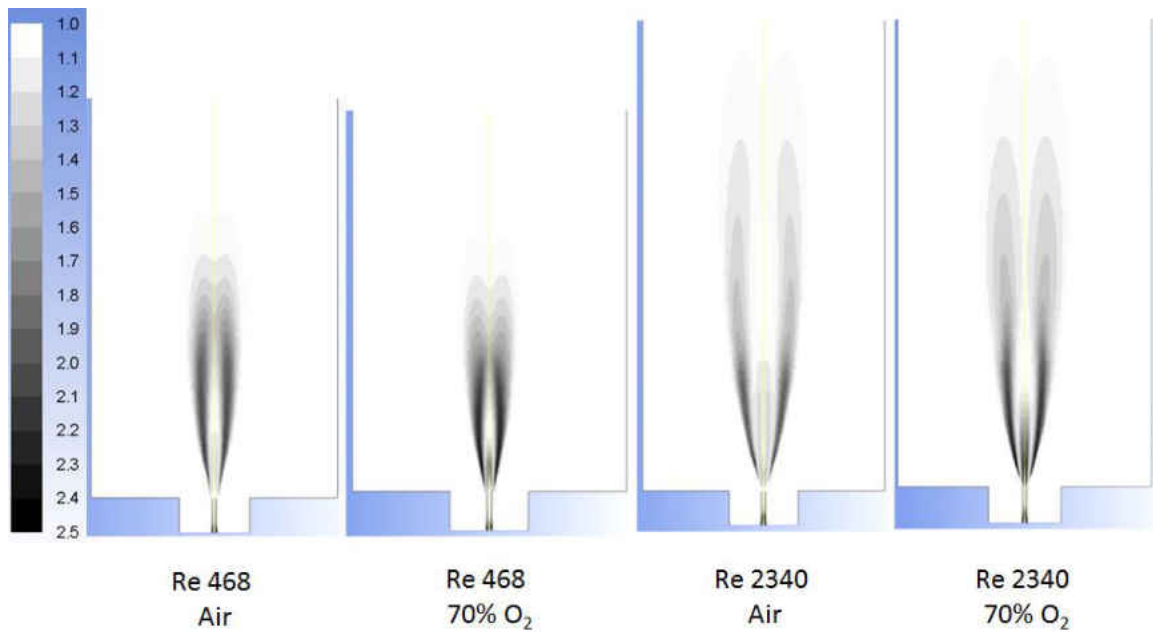


Figure 2-11: Emission enhancement due to TRI in different flames

2.5. Conclusions

An assessment of different radiation modeling strategies was carried out through simulations of twenty-four, laminar to transitional, air-methane and oxy-methane diffusion flames in a lab-scale furnace. User-defined functions were implemented for: gray and non-gray formulations of a recently proposed WSGG radiative property model for the gas-phase and a turbulence radiation interaction model for the temperature fluctuations. The effect of soot was also investigated by employing the Moss-Brookes soot model. The numerical predictions were compared against experimental measurements of: wall temperature, gas temperature, flame lengths and radiant fractions. The results lead to the following conclusions:

1. By modeling the gas-phase chemistry using the non-adiabatic extension of the equilibrium based mixture fraction approach, an adequate agreement was obtained between the numerical predictions and experimental measurements of the gas and wall temperatures.

These temperature predictions however were not sensitive to the gas radiative property model.

2. Numerical predictions of the flame length determined through the axial profiles of OH were in good agreement against the experimental measurements. The numerical predictions confirmed with the experimental observations of: increase in flame lengths with increase in fuel-inlet Reynolds numbers and a decrease in flame length with the increase in O₂ composition in the oxidizer stream attributed to a decrease in stoichiometric mixture fraction at higher O₂ compositions that displaces the locus of flame front to regions where a lower degree of mixing has been achieved. The flame length predictions were also not sensitive to the radiative property model employed in the calculations.

3. The radiant fractions of the flames were numerically estimated from the surface integral of the incident radiative fluxes along the side furnace walls. The radiant fraction was experimentally determined through line-of-sight measurements of wall temperature, gas temperature and radiatively participating gases employing the SNB model RADCAL. The methodological differences between the experimental and numerical approaches precluded a direct comparison of the two radiant fraction estimates. However, the observed experimental trends of increase in radiant fractions with the increase in Reynolds numbers and oxygen concentrations were numerically replicated. The non-gray model calculations predicted a lower radiant fraction than the gray model calculations with the variations between the gray and non-gray model predictions increasing with decrease in Reynolds numbers. This is attributed to sharper temperature gradients encountered in the smaller flames at lower Reynolds numbers. The effect of soot in the simulations was assessed by employing the Moss-Brookes soot model. At a given oxidizer composition, the computed soot volume

fractions were found to increase with increase in Reynolds numbers due to shorter residence times and incomplete mixing. However, with the increase in oxygen concentrations in the oxidizer, the soot volume fraction decreases due to the increase in oxidation rate of soot by the OH radicals. As a result of the low soot volume fractions predicted in the simulations, the presence of soot had a negligible effect on the radiant fraction predictions in these methane diffusion flames.

4. A preliminary investigation of TRI was carried out by assuming that the effect of TRI was dominated by the fluctuations in the temperature or the temperature self-correlation term. The emission enhancement due to the temperature fluctuations was found to be localized to the flame sheet. As a result, including the TRI model did not affect our radiative flux predictions.

2.6. References

- [1] G. Krishnamoorthy, A new weighted-sum-of-gray-gases model for oxy-combustion scenarios, *International Journal of Energy Research* (2012) doi: 10.1002/er.2988
- [2] C. Yin, L.C.R. Johansen, L.A. Rosendahl, S.K. Kær, New weighted sum of gray gases model applicable to computational fluid dynamics (CFD) modeling of oxy–fuel combustion: derivation, validation, and implementation, *Energy & Fuels* 24 (2010) 6275-6282.
- [3] R. Johansson, K. Andersson, B. Leckner, H. Thunman, Models for gaseous radiative heat transfer applied to oxy-fuel conditions in boilers, *International Journal of Heat and Mass Transfer* 53 (2010) 220-230.

- [4] T. Kangwanpongpan, F. H. França, R. Corrêa da Silva, P.S. Schneider, H. J. Krautz, New correlations for the weighted-sum-of-gray-gases model in oxy-fuel conditions based on HITEMP 2010 database. *International Journal of Heat and Mass Transfer* 55 (2012) 7419-7433.
- [5] C. Yin, L.A. Rosendahl, S.K. Kær, Chemistry and radiation in oxy-fuel combustion: A computational fluid dynamics modeling study, *Fuel* 90 (2011) 2519-2529.
- [6] S. Hjartstam, R. Johansson, K. Andersson, F. Johnsson. Computational Fluid Dynamics Modeling of Oxy-Fuel Flames: The Role of Soot and Gas Radiation, *Energy and Fuels* 26 (2012) 2786-2797.
- [7] S. Hjartstam, F. Normann, K. Andersson, F. Johnsson. Oxy-fuel combustion modeling: performance of global reaction mechanisms, *Industrial Engineering and Chemistry Research* 51 (2012) 10327–10337.
- [8] V. Bechera, S. Clausen, A. Fateev, H. Spliethoff. Validation of spectral gas radiation models under oxyfuel conditions. Part A: Gas cell experiments, *International Journal of Greenhouse Gas Control* 5S (2011) S76–S99.
- [9] C. Yin. Nongray-gas effects in modeling of large-scale oxy–fuel combustion processes. *Energy and Fuels* 26 (2012) 3349-3356.
- [10] P. Nakod, G. Krishnamoorthy, M. Sami, S. Orsino. A comparative evaluation of gray and non-gray radiation modeling strategies in oxy-coal combustion simulations, *Applied Thermal Engineering* 54 (2013) 422-432.
- [11] T. Kangwanpongpan, R.C. da Silva, H.J. Krautz, Prediction of oxy-coal combustion through an optimized weighted sum of gray gases model, *Energy* (2011) 1-8.

- [12] P. Edge, M. Gharebaghi, R. Irons, R. Porter, R.T.J. Porter, M. Pourkashanian, Combustion modelling opportunities and challenges for oxy-coal carbon capture technology, *Chemical Engineering Research and Design*, 89 (2011) 1470–1493
- [13] P. Edge, S.R. Gubba, L. Ma, R. Porter, M. Pourkashanian, A. Williams. LES modelling of air and oxy-fuel pulverised coal combustion—impact on flame properties, *Proceedings of the Combustion Institute* 33 (2011) 2709-2716.
- [14] V. Becher, J.P. Bohn, P. Dias, H. Spliethoff. Validation of spectral gas radiation models under oxyfuel conditions—Part B: Natural gas flame experiments, *International Journal of Greenhouse Gas Control* 5 (2011) S66-S75.
- [15] M. Ditaranto, T. Oppelt, Radiative heat flux characteristics of methane flames in oxy-fuel atmospheres, *Experimental Thermal and Fluid Science* 35 (2011) 1343-1350.
- [16] M. Ditaranto, T. Oppelt, L. Bard, I. Saanum, Radiation and stability of oxy-fuel combustion, *International conference on sustainable fossil fuels for future energy*, <http://www.co2club.it/agenda/Presentations/S4FE%20ditaranto.pdf> (last accessed on August 8th, 2013).
- [17] ANSYS FLUENT User's Guide, Version 12, ANSYS Inc., Canonsburg, PA, 2009.
- [18] H. Chu, F. Liu, H. Zhou. Calculations of gas thermal radiation transfer in one-dimensional planar enclosure using LBL and SNB models, *International Journal of Heat and Mass Transfer* 54 (2011) 4736–4745.
- [19] P. Glarborg, L.L.B. Bentzen, Chemical effects of a high CO₂ concentration in oxy-fuel combustion of methane, *Energy & Fuels* 22 (2007) 291-296.

- [20] A. Amato, B. Hudak, P. D'Souza, P. D'Carlo, D. Noble, D. Scarborough, J. Seitzman, T. Lieuwen, Measurements and analysis of CO and O₂ emissions in CH₄/CO₂/O₂ flames, *Proceedings of the Combustion Institute* 33 (2011) 3399–3405.
- [21] S.J. Brookes, J.B. Moss. Prediction of soot and thermal radiation in confined turbulent jet diffusion flames, *Combustion and Flame* 116 (1999) 486–503.
- [22] J. Andersen, C.L. Rasmussen, T. Giselsson, P. Glarborg, (2009). Global combustion mechanisms for use in CFD modeling under oxy-fuel conditions, *Energy & Fuels* 23 (2009) 1379-1389.
- [23] K. Bhadraiah, V. Raghavan. Numerical simulation of laminar co-flow methane–oxygen diffusion flames: effect of chemical kinetic mechanisms, *Combustion Theory and Modelling* 15 (2000) 23-46.
- [24] J.C. Sautet, L. Salentey, M. Ditaranto, J.M. Samaniego. Length of natural gas-oxygen non-premixed flames, *Combustion Science and Technology* 166 (2001) 131-150.
- [25] M. De Leo, A. Saveliev, L.A. Kennedy, S.A. Zelepouga. OH and CH luminescence in opposed flow methane oxy-flames, *Combustion and Flame* 149 (2007) 435–447.
- [26] R. Porter, F. Liu, M. Pourkashanian, A. Williams, D. Smith. Evaluation of solution methods for radiative heat transfer in gaseous oxy-fuel combustion environments, *Journal of Quantitative Spectroscopy and Radiative Transfer* 111 (2010) 2084–2094.
- [27] S.J. Brookes, J.B. Moss. Prediction of Soot and Thermal Radiation in Confined Turbulent Jet Diffusion Flames, *Combustion and Flame* 116 (1999) 486–503.
- [28] P.J. Coelho, O.J. Teerling, D. Roekaerts. Spectral radiative effects and turbulence/radiation interaction in a nonluminous turbulent jet diffusion flame, *Combustion and Flame* 133 (2003) 75–91.

- [29] P.J. Coelho. Detailed numerical simulation of radiative transfer in a nonluminous turbulent jet diffusion flame, *Combustion and Flame* 136 (2004) 481–492.
- [30] P.J. Coelho. Numerical simulation of the interaction between turbulence and radiation in reactive flows, *Progress in Energy and Combustion Science* 33 (2007) 311–383.
- [31] S.P. Burns. Turbulence radiation interaction modeling in hydrocarbon pool fire simulations, Sandia Rept. SAND99-3190, Sandia, New Mexico, (1999).

3. AN EXPERIMENTAL AND NUMERICAL STUDY OF CONFINED, LAMINAR, DIFFUSION, OXY-METHANE FLAMES

ABSTRACT

Experimental measurements and computational fluid dynamic (CFD) simulations of three, confined, laminar ($Re_{jet} 1404$), diffusion, methane flames in oxidizer compositions of: 21% O_2 – 79% N_2 , 35 % O_2 - 65% CO_2 and 50% O_2 – 50 % CO_2 are reported in this chapter. The accuracies of three gas-phase chemistry models were assessed by comparing their predictions against experimental measurements of temperature, specie concentrations and flame lengths. The chemistry was modeled employing the Eddy Dissipation Concept (EDC) employing a 41-step detailed chemistry mechanism, the non-adiabatic extension of the equilibrium Probability Density Function (PDF) based mixture-fraction model and a two-step global finite rate chemistry model with modified rate constants proposed to work well in oxy-methane flames.

Results from the EDC and equilibrium PDF models were in reasonable agreement against experimental measurements of O_2 , CO_2 and gas temperature at all oxidizer compositions. However, all three models failed to adequately predict the CO concentrations. Both the EDC and equilibrium PDF models correctly predicted increases in CO, OH and O concentrations with increase in oxygen concentration in the oxidizer. When flame lengths

were determined by the axial OH concentrations, the equilibrium PDF model predictions agreed more closely with experimental observations compared to those from the EDC model. An investigation into the importance of the Soret effect revealed that thermal diffusion affects the temperature and peak OH and CO concentrations in the fuel rich regions with its impact increasing with oxidizer oxygen concentrations and flame temperatures. However it does not have a significant impact on the predicted flame lengths.

Based on the results from this study, the equilibrium PDF model in conjunction with a high-fidelity non-gray model for the radiative properties of the gas-phase may be deemed as accurate to capture the major gas species concentrations, temperatures and flame lengths in oxy-methane flames with long chemical residence times whereas simulations employing detailed chemistry mechanisms that take into effect thermophoresis need to be developed/validated to accurately predict pollutant concentrations such as CO, NO_x and soot.

3.1. Introduction

3.1.1. Oxy-methane combustion chemistry

In terms of the gas phase chemistry during oxy-combustion of methane which is the focus of this study, the primary impact of an oxy-combustion atmosphere is the participation of CO₂ through the reaction: $\text{CO}_2 + \text{H} \rightleftharpoons \text{CO} + \text{OH}$. This could result in the CO₂ in the oxidizer stream competing with O₂ for the atomic hydrogen through the equilibrium reaction: $\text{CO}_2 + \text{H} \rightleftharpoons \text{CO} + \text{OH}$ and result in the formation of more CO especially in the near burner region [1]. Although the high CO concentrations initially formed eventually gets oxidized, Amato et al [2] concluded that the CO₂ and H destruction reactions along with the destruction of O₂ through the reaction $\text{O}_2 + \text{H} \rightleftharpoons \text{O} + \text{OH}$ were the key reactions controlling

the concentrations of CO₂ and O₂ in the post-flame zone. While high local concentrations of CO may contribute to the near-burner corrosion, high O₂ concentrations in the flue gases translate to higher costs associated with the generation of a pure O₂ stream. Furthermore, accurate predictions of the H, O and OH concentrations are also critical for predicting the NO_x and soot concentrations in oxy-flames as these radicals control the oxidation and reduction of these pollutants [3 - 5].

Gas-phase radiative property models in the form of weighted-sum-of-gray-gases (WSGG) coefficients based on different spectroscopic databases [6-9] have been proposed and validated in some instances against line-by-line benchmark calculations. Similarly, the kinetic parameters in previously proposed 2-step and 4-step global kinetic mechanisms for methane combustion [10, 11] have been refined and employed in oxy-combustion scenarios [12 - 14]. Table 3-1 summarizes the results from CFD simulations of oxy-methane/natural gas combustion employing these refined chemistry and radiation models.

Table 3-1: A summary of previous CFD studies of oxy-methane/natural gas combustion.

Reference	System	Chemistry models	Radiation Modeling	Results and Conclusions
Prieler et al [15]	Turbulent high temperature furnace for smelting and annealing applications	Eddy dissipation concept (EDC) with 46 reversible reactions, steady laminar flamelet (SFM) approach with flamelet libraries generated employing 25-step, 46-step mechanisms as well as 325 reactions in GRI-Mech3.0	Default WSGGM in ANSYS FLUENT (gray model) employed with P-1 and Discrete Ordinates (DO) radiation models	Temperature and species concentration predictions from EDC and SFM were very similar. SFM calculations were about 5 times faster than the EDC calculations that employed detailed chemistry. The P1 radiation model over-estimated emission and predicted lower temperatures than measurements
Nemittallah and Habib [16]	Turbulent, diffusion flame in a gas-turbine combustor investigated for a wide range of operational parameters	Modified 2-step chemistry mechanism [12]	DO radiation model; Radiative property model was not specified	Overall flame shape and exhaust gas concentrations were well-predicted employing the modified two-step mechanisms
Galetti et al [17]	3 MW semi-industrial burner	Eddy Dissipation Model (EDM), EDC, modified global mechanisms	P1/DO, revised WSGGM coefficients [6]	Turbulence Chemistry interactions play an important role in determining the temperature and species concentrations, EDC provides satisfactory temperature and species predictions
Wheaton et al [18]	0.8 MW turbulent burner, High Temperature air combustion (HTAC) burner	Non-adiabatic equilibrium PDF	DO radiation model, revised WSGGM [25] employed in non-gray simulations	Reasonable agreement of temperature with measurements, high concentrations of radiatively participating gases by themselves are not enough to warrant the use of non-gray models. The peak temperatures, temperature gradients and furnace dimensions also need to be taken into consideration
Yin [13]	Semi-industrial furnace	Global 2-step and 4-step reaction mechanisms [10, 11] as well as modified versions of these mechanisms	DO radiation model, revised WSGGM [7] employed in gray simulations	The refined chemistry models were able to better predict the temperature and CO concentrations downstream of the furnace
Bhadriah and Raghavan [19]	laminar, unconfined	4 global mechanisms, 43-step skeletal mechanism	Optically thin radiation model	Major gases and temperature predictions from the 2-step are closer to the 43-step mechanism. 2- step predicts the location of the reaction zone accurately. Improvements agree at higher flow rates but only qualitative prediction of CO
Kim et al. [20]	0.78 MW turbulent natural gas furnace	Conservative conditional moment closure for turbulence chemistry interactions with detailed chemistry mechanisms	Radiation model and the determination of radiative properties not specified	A good qualitative agreement is obtained with the temperature over-estimated at short radial distances. CO ₂ was under-estimated and CO was over-estimated in the high temperature regions
Bennett et al. [21]	laminar, unconfined diffusion flames	GRI-Mech 3.0	Optically thin radiation model	Computational and experimental flame lengths and maximum centerline temperatures show excellent agreement. Radial profiles when plotted at fixed values of a dimensionless axial co-ordinate also show excellent agreement
Abdul-Sater and Krishnamoorthy [22]	laminar, confined diffusion flames	Non-adiabatic equilibrium PDF	DO radiation model, revised WSGGM [25] employed in gray and non-gray simulations	Computational and experimental flame lengths and temperature profiles show excellent agreement. Significant variations in the flame radiant fraction predictions between the gray and non-gray models

Most of the investigated systems are turbulent and at a semi-industrial scale where the predictions are impacted by the interplay and accuracies of the turbulence, radiation and the chemistry models. Furthermore, while global chemistry models were deemed to be accurate in industrial applications, detailed chemistry models that account for dissociation

were found to be necessary to accurately predict pollutant formation. In order to carry out a rigorous assessment of chemistry models in oxy-combustion scenarios, experimental and numerical results from three, confined, laminar, diffusion methane flames are reported in this study. By considering a laminar system we minimize the impact of turbulence and the uncertainties associated with turbulence models. In a previous study we had carried out an assessment of radiation models in these flames by comparing the predictions from gray and non-gray radiation models against experimental measurements of radiant fractions and flame lengths [22]. By employing a soot model in that study we had determined that the impacts of soot and its influence on the temperature measurements were minimal and the soot concentrations only decreased with increase in oxygen concentration in the oxidizer.

3.2. Experimental Conditions

Geometric details of the furnace and flow boundary conditions associated with the oxy-flames reported in this study may be found in Ditaranto and Oppelt [23] and is only briefly described here. The furnace consists of a fuel nozzle of diameter 5 mm, oxidizer nozzle of diameter 100 mm enclosed in combustion chamber of 350 mm and 100 mm in length with stainless steel walls. The large dimension of the furnace relative to that of the flame minimized interaction and perturbation of the flow with the wall. The oxidizer gas was sent through a series of perforated plates to ensure uniform velocity distribution. The inside faces of the stainless steel walls of the reactor were coated with a blackbody paint of emissivity 0.98. The temperature and gas concentration (CO_2 , O_2 , and CO) profiles around the flames were measured at different axial heights and in a radial direction from the wall until the vicinity of the outer limit of the flame as defined as when the CO concentration

increased sharply. Local gas was sampled with a quartz probe and analyzed with conventional gas analyzers and the temperature profiles were obtained by transversing radially four equally spaced 500 μm fine bead thermocouples in the gas layer. In this study, experimental measurements of temperature and major chemical species (CO_2 , O_2 , and CO) are reported for three laminar flames with oxidizer compositions of 35% and 50% O_2 in CO_2 as well as air at a fuel Reynolds number of 1404. Obtaining reliable species profiles within the flames in small laboratory flames requires non-intrusive laser diagnostics, which were not applied in this study. The usage of the sampling probe was therefore been limited to regions where its measurements could be trusted.

The co-flow velocity and fuel velocity were maintained at 0.25 m/s and 4.6 m/s, respectively. The inlet temperature of the fuel was maintained at 288 K for the fuel densities to match the fuel inlet Reynolds number of 1404. The temperature of the CO_2 supply was observed to be strongly dependent on the flow rate and the pressure in the liquid CO_2 container due to its sensitivity to Joule-Thomson effects. Consequently, some temperature fluctuations in the co-flow plenum were observed and an average co-flow temperature of 288 K was therefore employed in the simulations. Although these variations in the co-flow temperatures can strongly influence local flame extinction and lift-off characteristics, they were anticipated to play a minimal impact on the results and conclusions reported in this study.

3.3. CFD Modeling Approach

3.3.1. Geometry and Mesh

The CFD simulations were carried out using the commercial code ANSYS FLUENT

[24]. The furnace was modeled in a 2D axisymmetric domain to take advantage of the symmetry of the problem. The geometry was meshed employing 30,700 hexahedral control volumes. Further refinement of the mesh to 263,000 control volumes did not change the results reported in the study. The flames in this study were determined to be in the buoyant regime since their laminar Froude numbers were less than unity [23]. Therefore, the pressure-velocity coupling was accomplished using the SIMPLEC algorithm which we have determined from past experience to perform well in such buoyancy driven enclosure flows. The PRESTO and QUICK schemes were employed for the spatial discretization of the pressure and momentum terms respectively since hexahedral cells were employed in the calculations [24]. Strong recirculation patterns were observed numerically and experimentally (via a decrease in gas temperature close to the walls as a result of downward flow). Therefore, in order to obtain steady-state converged results in the CFD simulations to compare against experimental measurements necessitated the utilization of the standard k - ϵ turbulence model. Furthermore, simulations of flames with fuel Reynolds numbers in the range Re 468 to Re 2340 are reported in this study and the utilization of the standard k - ϵ turbulence model ensured consistency in the modeling procedure across all the flames investigated in this study. Furthermore the values of y -plus along the boundaries indicated that the flow was being well resolved. Investigations of turbulence-radiation interactions in these flames along with the very low values of the mixture fraction variance computed outside the flames in the simulations reported in chapter 2 also re-affirm that the utilization of a turbulence model in the simulations has very little bearing on the results and conclusions reported in this chapter.

3.3.2. Radiation Modeling and Boundary Conditions

The radiation was modeled by solving the radiative transport equation (RTE) employing the Discrete Ordinate (DO) model. The angular discretization was carried out by employing a 4 x 4 theta x phi discretization. The adequacy of this angular resolution was established by determining that the reported variables did not change with any further increase in angular resolution. To determine the radiative property of the gas mixture, a recently proposed WSGG model [8] that is based on the Statistical Narrow Band Model RADCAL was implemented as a user-defined function (UDF) and employed in the combustion simulations. The WSGG model accurately calculates the radiative properties of CO₂ and H₂O vapor mixtures that are encountered in scenarios encompassing methane, natural gas or coal combustion under air-fired and oxy-fired conditions. Non-gray formulations (with five gray gases) of the WSGGM were employed in this study [8, 25].

For boundary conditions for the radiation model, the stainless steel walls of the reactor were assigned an emissivity of 0.98 at the inside walls of the reactor [23]. The external walls (assigned an emissivity of 0.7) were assumed to radiate to the ambient air at 300 K and the reactor wall temperature was established by an energy balance between the net radiative and convective heat fluxes at the inside walls of the reactor and the net emission from the outside wall of the reactor. The non-availability of the steady-state wall temperature profiles for all the flames necessitated the adopting of a physically realistic thermal boundary condition. The utilization of these boundary conditions has been validated in our previous study [22]. An additional set of simulations was carried out employing a constant wall temperature of 350 K. The reported results in this study did not change significantly as a result of the change in wall boundary conditions and does not alter our conclusions in

anyway.

3.3.3. Chemistry Modeling

Based on the recent studies summarized in Table 3-1, it is evident that particular attention is needed when choosing the turbulent-chemistry interaction and the kinetic mechanism to be used when simulating an oxy-methane flame. The turbulence-chemistry interaction could be accounted for employing several approaches such as: the Eddy Dissipation Concept (EDC), the laminar flamelet model and the equilibrium PDF based mixture-fraction model. In this study, the EDC, finite rate chemistry (FR) and equilibrium PDF models were used to solve for the combustion chemistry.

In the EDC model, chemical reactions are assumed to take place in small turbulent structures referred to as fine scales. This is based on the turbulent energy cascade where large eddies break up into smaller eddies. The fine scales are then treated as constant pressure reactors where the combustion occurs. The concentration of species is then calculated by integrating the chemistry within these fine scales. This is undertaken by modeling the volume fraction of these fine structures in which the reactions take place, the time-scale for mass transfer from the fine structure to the surrounding fluid as functions of the turbulent kinetic energy (k) and turbulent dissipation rates (ϵ). However, the validity of the EDC model is limited to turbulent Reynolds numbers greater than 64 [26, 27]. The turbulent Reynolds number is a function of the fluid density, distance to the near wall, turbulent kinetic energy and the laminar viscosity of the fluid [24]. Due to the small flame lengths encountered in this study, the turbulent Reynolds numbers were greater than 64 in the majority of the furnace and within the flame. However, there were regions just outside

the flame and in a thin section close to the wall where this requirement was not met. The implications of this on the CO predictions are discussed later. In this study, Smooke's skeletal mechanism [28] for methane combustion which consists of 33 reactions and 17 species was used to represent the chemistry associated with the EDC model. The k and ϵ turbulence terms are used to solve for the size of the fine scales and the chemical residence time.

In chapter 2, we had deemed the appropriateness of employing the non-adiabatic formulation of the equilibrium PDF based mixture-fraction model (denoted as PDF) for these buoyant enclosure flames. The flame length and temperature predictions were found to agree well with the experimental measurements as well as trends at different oxidizer compositions and fuel inlet Reynolds numbers. In the mixture fraction approach, the instantaneous thermochemical state of a fluid is related to its mixture fraction and its enthalpy. The benefits of this model is that by assuming equal species diffusivities, the individual species conservation equations reduce to a single "sourceless" conservation equation for the mixture fraction as a result of the cancellation of the reaction source terms in the species equations due to elemental conservation. This enabled us to estimate the concentrations of minor species such as OH as well as get accurate predictions of the flame temperature in a computationally efficient manner without the need to resort to a detailed chemical mechanism that is applicable to oxy-combustion conditions. Under the assumption of chemical equilibrium, all thermochemical scalars (species fractions, density, and temperature) are uniquely related to the mixture fraction(s) and the value of each mass fraction, density and temperature were determined from calculated values of mixture fraction, variance in mixture fraction and the enthalpy. Twenty chemical species were

considered in the equilibrium calculations (CH_4 , C_2H_2 , CH_3 , C_2N_2 , C_2H_6 , C_2H_4 , C_4H_2 , C_3H_3 , HNC , C(s) , CO , CO_2 , H_2O , OH , N_2 , O_2 , H , O , HO_2 and H_2). An assumed shape probability distribution function (PDF) was employed to describe any turbulence-chemistry interactions where the average value of the scalars is related to their instantaneously fluctuating values. In this study, the shape of the PDF was described by the beta function. 80 points in the mixture fraction and variance in mixture fraction space and 121 points in the enthalpy space were employed to carry out the interpolations and integrations within the PDF model.

The FR chemistry modeling in this study was carried out employing the global kinetic parameters reported for the Westbrook and Dryer (WD) mechanism in Yin et al. [13]. The original unmodified kinetic parameters [24] were employed in the methane-air flame whereas the modified rate constants were employed in the oxy-methane flame simulations.

3.4. Results and Discussion

Radial measurements of temperature, CO , CO_2 and O_2 outside the flame region were made at several axial locations in the three flames and are reported in this study. The CFD predictions are then compared against the experimental results.

3.4.1. Temperature

Figure 3-1 to Figure 3-3 compare the numerical temperature predictions against experimental measurements along the radial direction at four different axial locations for both air and oxy- combustion cases. The axial centerline ($r = 0$) corresponds to the flame center. The experimentally measured flame lengths in these flames were reported to be 482 mm, 434 mm and 373 mm respectively. In Figure 3-1, predictions from all three chemistry models are seen to agree well against experimental measurements. Variations

between the models are more pronounced at lower axial and radial distances closer to the centerline axis. The finite rate (FR) chemistry model by virtue of limited dissociation predicts higher temperature than the PDF and EDC based approaches. The EDC based approach incorporates multiple minor species that may have slower rates of formation and are not yet at their equilibrium concentrations at smaller residence times or lower axial distances. Hence, its temperature predictions are also slightly higher than the equilibrium PDF approach at lower axial distances. However, predictions from all 3 models start converging to the same values at large residence times in the post-flame zone when all of the combustion products attain equilibrium as well as in the fuel lean regions outside the flame. The trends in the temperature predictions in the oxy-flames shown in Figure 3-2 and Figure 3-3 are consistent with those observed in Figure 3-1. In the oxy-flames, the models converge to the same temperature values at lower axial distances since the flame lengths are shorter and decrease with an increase in oxygen concentration in the oxidizer stream [22]. The equilibrium based mixture fraction and EDC models show a slightly better agreement with experimental measurements outside the flame.

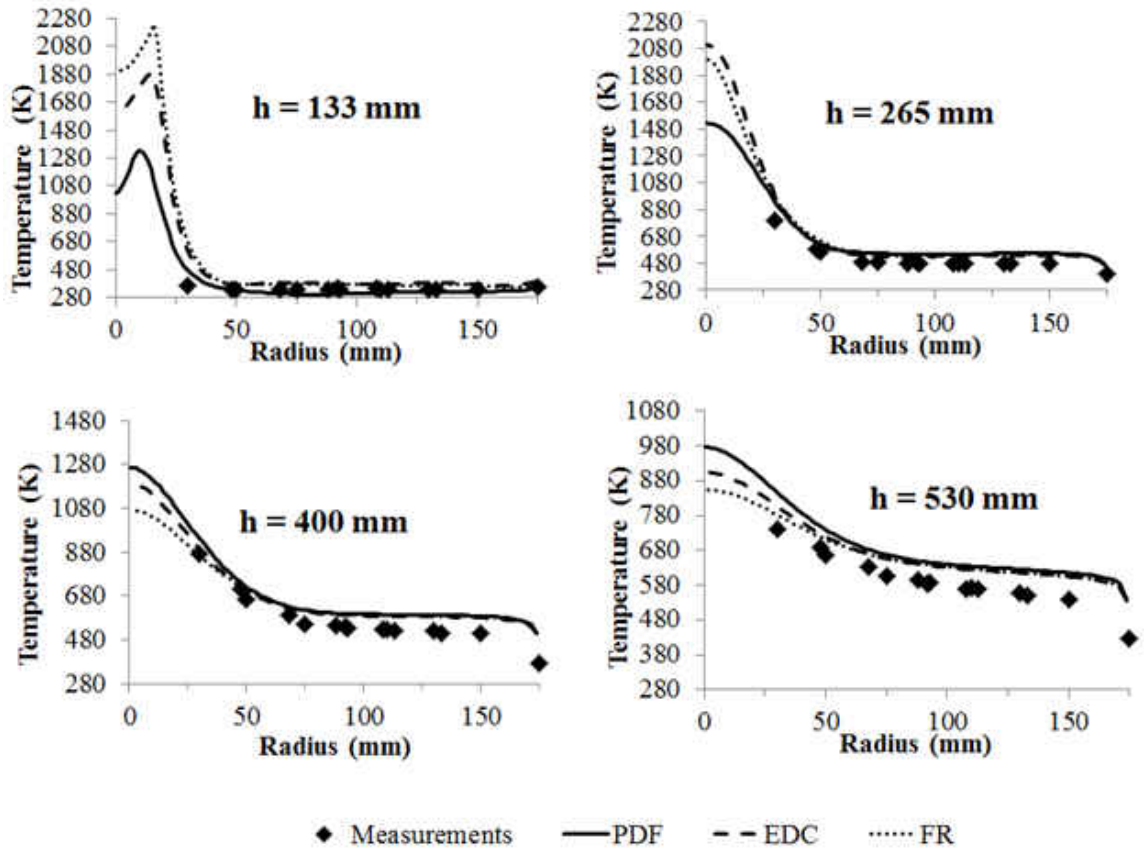


Figure 3-1: Radial temperature profiles at different axial locations for the air-methane flame

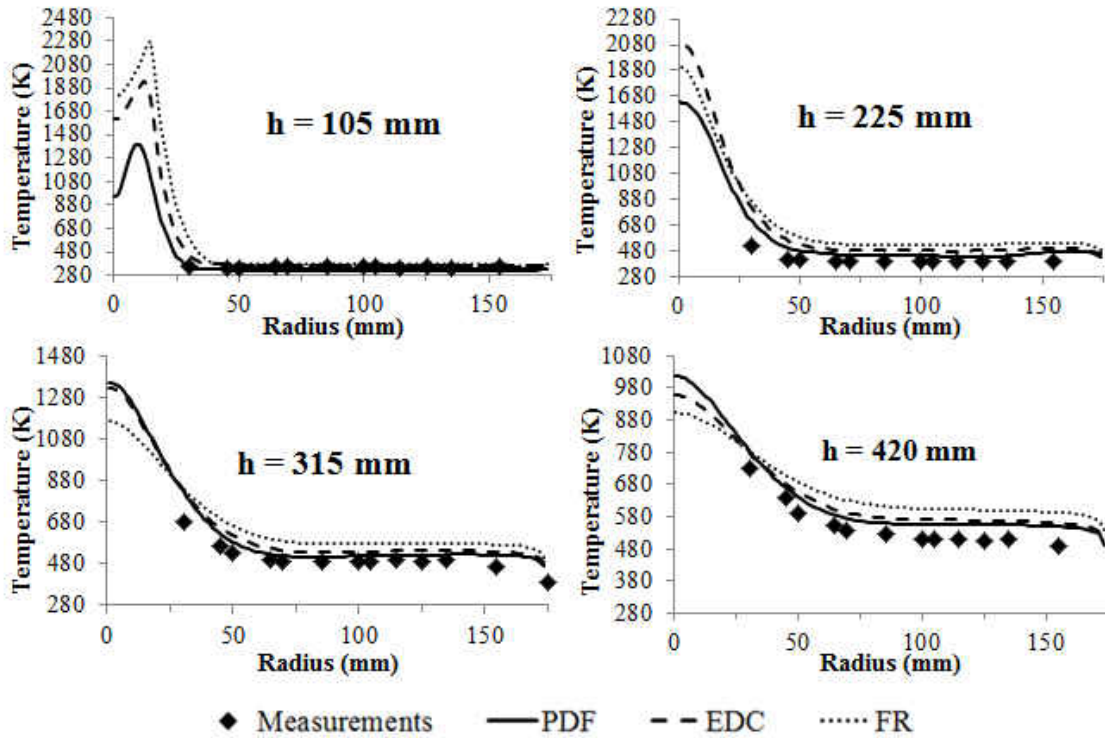


Figure 3-2: Radial temperature profiles at different axial locations for the Oxy-methane flame (35% O₂ - 65% CO₂).

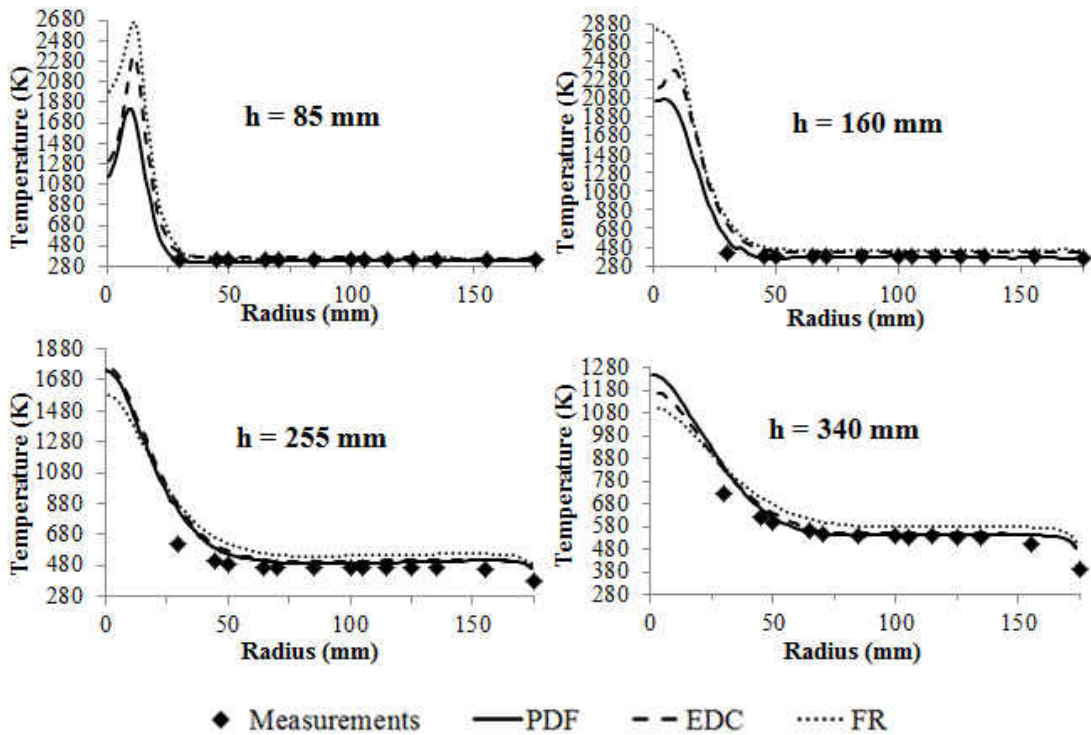


Figure 3-3: Radial temperature profiles at different axial locations for the Oxy-methane flame (50% O₂ - 50% CO₂).

3.4.2. CO₂

Figure 3-4 to Figure 3-6 compare the numerical variations in CO₂ concentrations (mol % dry basis) against experimental measurement along the radial direction at four different axial locations for both air and oxy-fuel combustion cases. Corresponding to the temperature plot, the finite rate chemistry model over-predicts the CO₂ at lower axial distances and therefore at small flame residence times whereas the EDC and PDF models converge to the correct value at large residence times. The finite rate chemistry model with the modified WD rate constants while performing well in the 35 % O₂ – 65 % CO₂ oxy-flame, over-predicts the CO₂ concentrations in the 50 % O₂ – 50 % CO₂ oxy-flame.

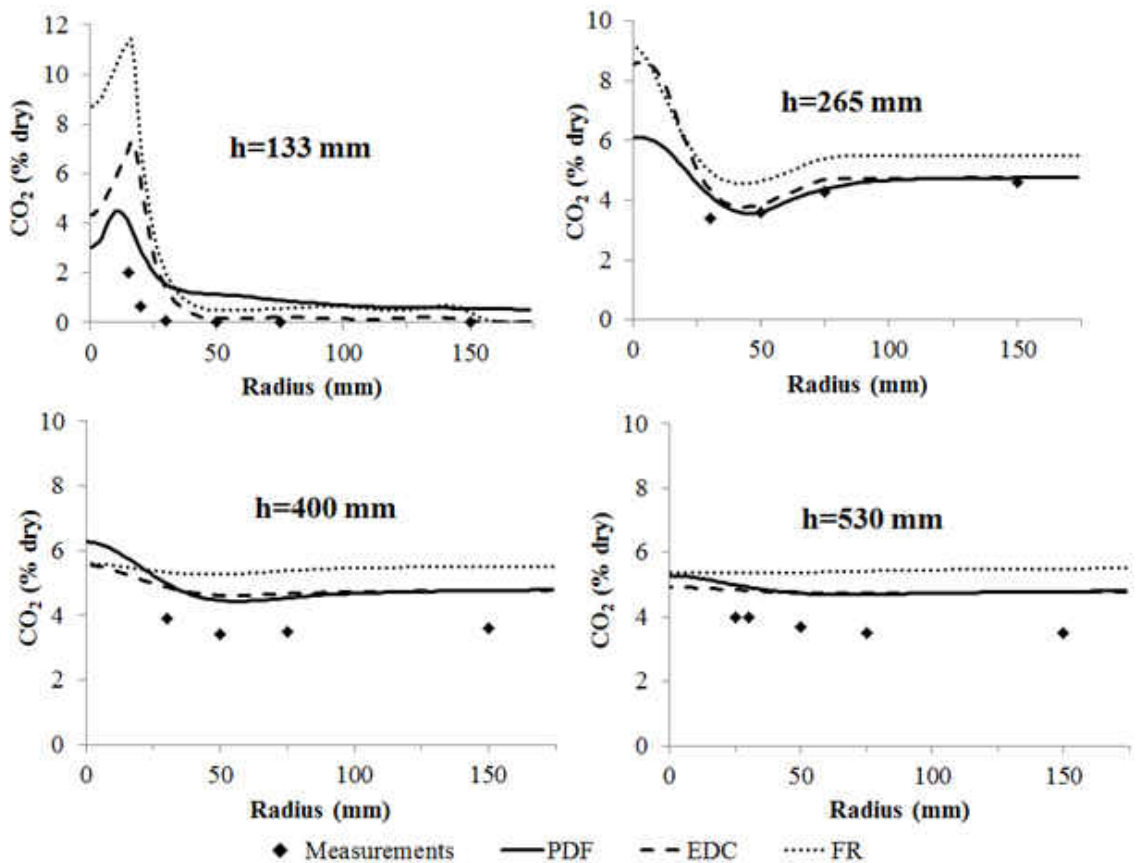


Figure 3-4: Radial CO₂ profiles at different axial locations for the air-methane flame.

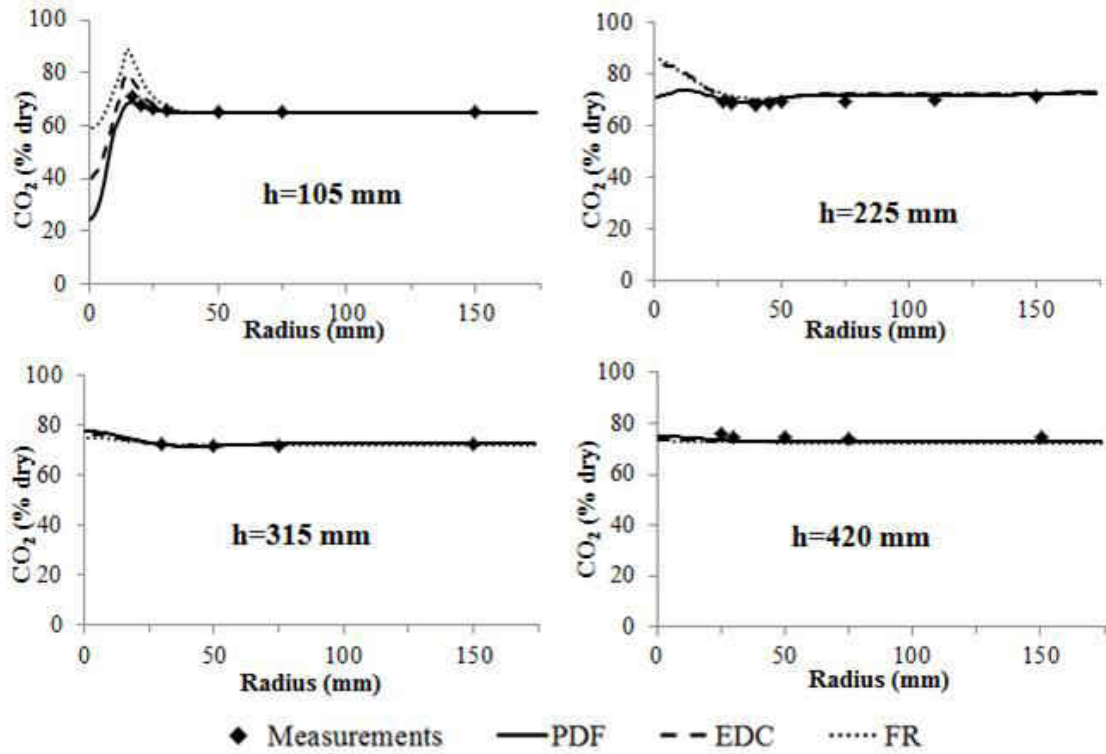


Figure 3-5: Radial CO₂ profiles at different axial locations for the oxy-methane flame (35% O₂ - 65% CO₂).

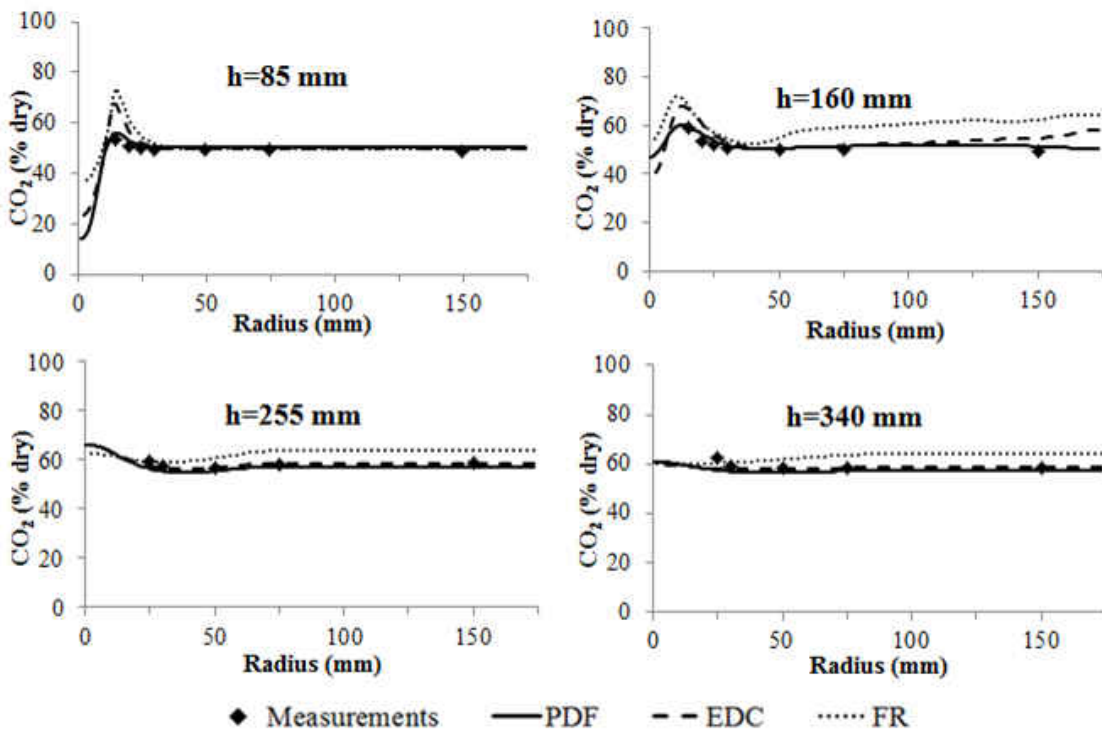


Figure 3-6: Radial CO₂ profiles at different axial locations for the oxy-methane flame (50% O₂ - 50% CO₂).

3.4.3. O₂

Figure 3-7 shows the predicted radial variations in the O₂ concentrations (mol % dry basis) against experimental measurements. While reasonable agreement with the experimental predictions is obtained from the EDC and equilibrium PDF based approaches, the finite rate chemistry model with the modified WD rate constants while performing well in the 35 % O₂ – 65 % CO₂ oxy-flame, under-predicts the O₂ concentrations in the 50 % O₂ – 50 % CO₂ oxy-flame.

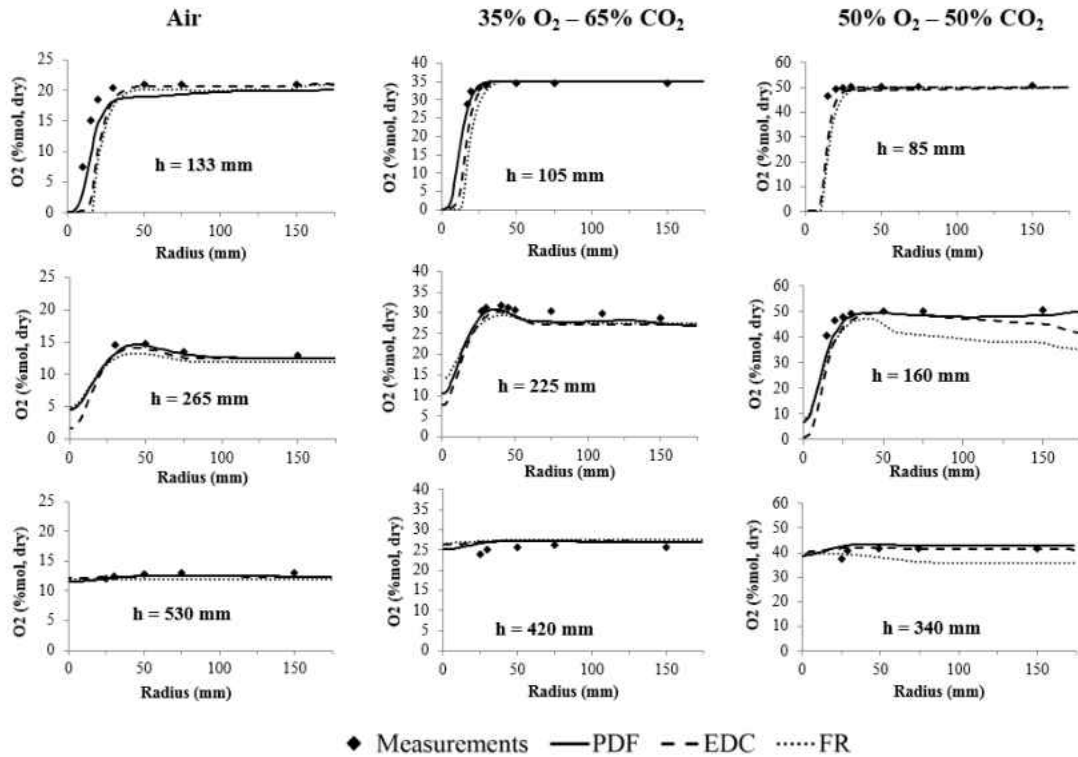


Figure 3-7: Radial O₂ profiles at different axial locations for the air and oxy-flames investigated in this study.

3.4.4. CO

Figure 3-8 shows the predicted radial variations in the CO concentrations (ppm dry basis) against experimental measurements. First, predictions from all chemistry models do

not agree well against experimental measurements. While all three models, correctly predict high CO concentrations in the fuel-rich regions within the flame, only the EDC model predicts CO in the fuel-lean regions outside the flame. The EDC model predictions however are more than an order of magnitude higher than the experimental measurements. We believe that this is a consequence of employing the EDC model in those localized regions outside the flame where the turbulent Reynolds number was less than 64. The equilibrium CO emissions in oxy-combustion systems are largely determined by the equilibrium $\text{CO} + \text{OH} \leftrightarrow \text{CO}_2 + \text{H}$. Therefore, predicting the radical concentrations is critical to obtaining accurate estimates of CO.

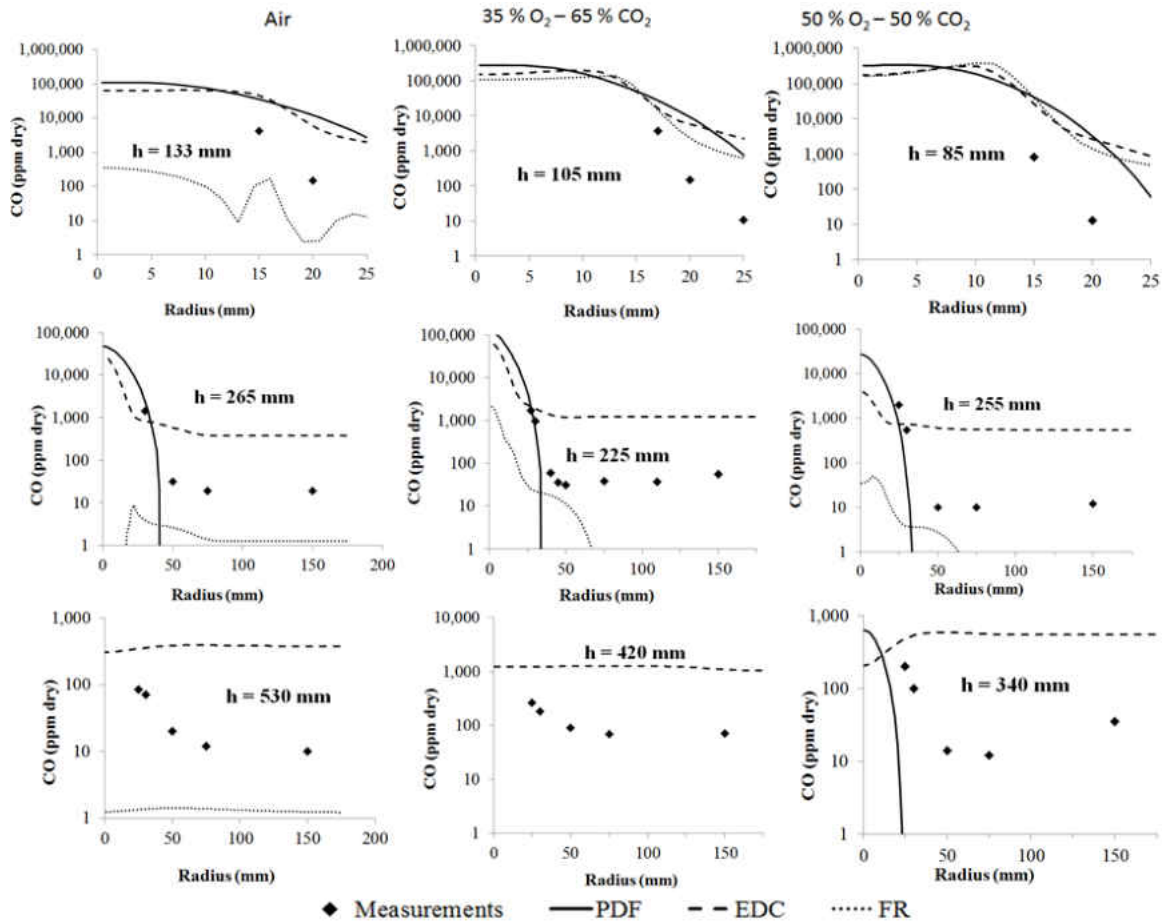


Figure 3-8: Radial CO profiles at different axial locations for the air and oxy-flames investigated in this study.

A hybrid EDC-FR kinetics model that calculates an effective reaction rate by appropriating weighting the laminar FR reaction rate and the turbulent reaction rate depending on the local turbulent Reynolds number of the flow was recently proposed by Shienejadhesar et al. [28]. In the methane-air flames that were investigated, the hybrid model was shown to improve estimates of radicals in comparison to the standard EDC model when they were both compared against experimental measurements. We believe that an improved agreement in CO predictions may be obtained by the hybrid model or by employing a more

detailed chemistry mechanism as demonstrated by Bennett et al. [21] (cf. Table 3-1).

The equilibrium $\text{CO} + \text{OH} \leftrightarrow \text{CO}_2 + \text{H}$ also implies that higher CO_2 concentrations, lead to larger equilibrium CO emissions. This trend is reflected in the axial variations in CO predicted by the chemistry models shown in Figure 3-9 for the three flames. The predictions from the global finite rate chemistry model with modified WD rate constants are seen to be comparable to those of the equilibrium mixture fraction and EDC model predictions in the oxy-flames along the fuel-rich axial centerline. This is in agreement with those of Anderson et al. [12] and Yin et al. [13] where an improved temperature and CO agreement was obtained with the refined global chemistry mechanisms.

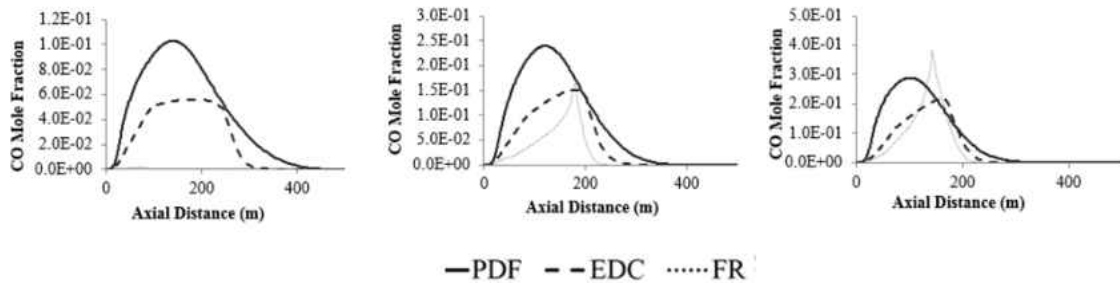


Figure 3-9: Axial CO profiles for the air and oxy-flames investigated in this study.

3.4.5. OH and Flame Lengths

Experimentally determined luminescence from the OH radical is often employed to determine flame lengths. Furthermore, the concentrations of pollutants such as NO_x and soot are greatly determined by OH concentrations. In oxy-combustion scenarios an increase in OH concentrations with an increase in CO_2 in the oxidizer stream is expected as per the reaction $\text{CO} + \text{OH} \leftrightarrow \text{CO}_2 + \text{H}$ in the fuel rich regions [5]. Similarly, OH concentration increase with increase in O_2 concentration in the oxidizer stream is also expected as a result

of the $O_2+H \leftrightarrow O+OH$ reaction. However, it is important to note that in the oxy-flames investigated in this study, an increase in O_2 concentrations in the oxidizer is accompanied by a corresponding decrease in the CO_2 concentrations.

Figure 3-10, compares the centerline predictions of the OH radical in the three flames investigated in this study. An increase in the oxidizer O_2 concentrations in the oxy-flames results in a corresponding increase in the OH concentrations which is consistent with the observations in previous studies [23, 29]. The gradients in the OH concentrations along the flame axis are higher along with peak values in the EDC calculations compared against the equilibrium PDF approach. Figure 3-11, compares the numerical predictions of the flame lengths by the EDC and equilibrium PDF approaches as determined by the axial location where the OH concentration approximately reaches zero compared against experimental measurements. While both the equilibrium PDF and EDC models replicate the experimental observations of a decrease in flame lengths with increase in O_2 concentrations, the agreement is with experiments is better with the equilibrium PDF approach. The EDC model predictions results in an under-prediction of the flame lengths.

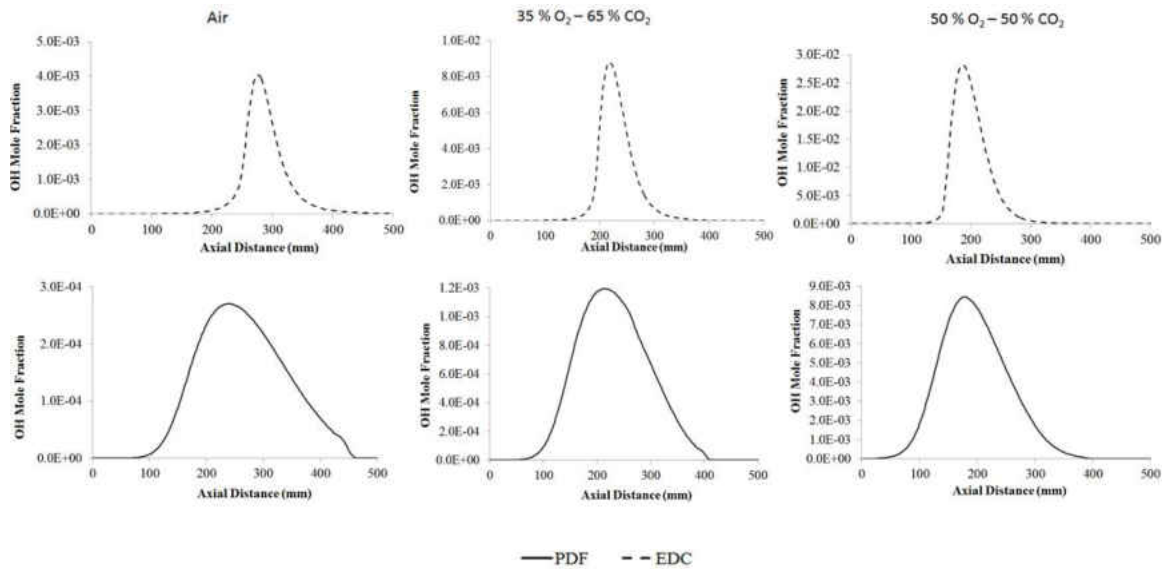


Figure 3-10: Axial OH profiles for the air and oxy-flames investigated in this study.

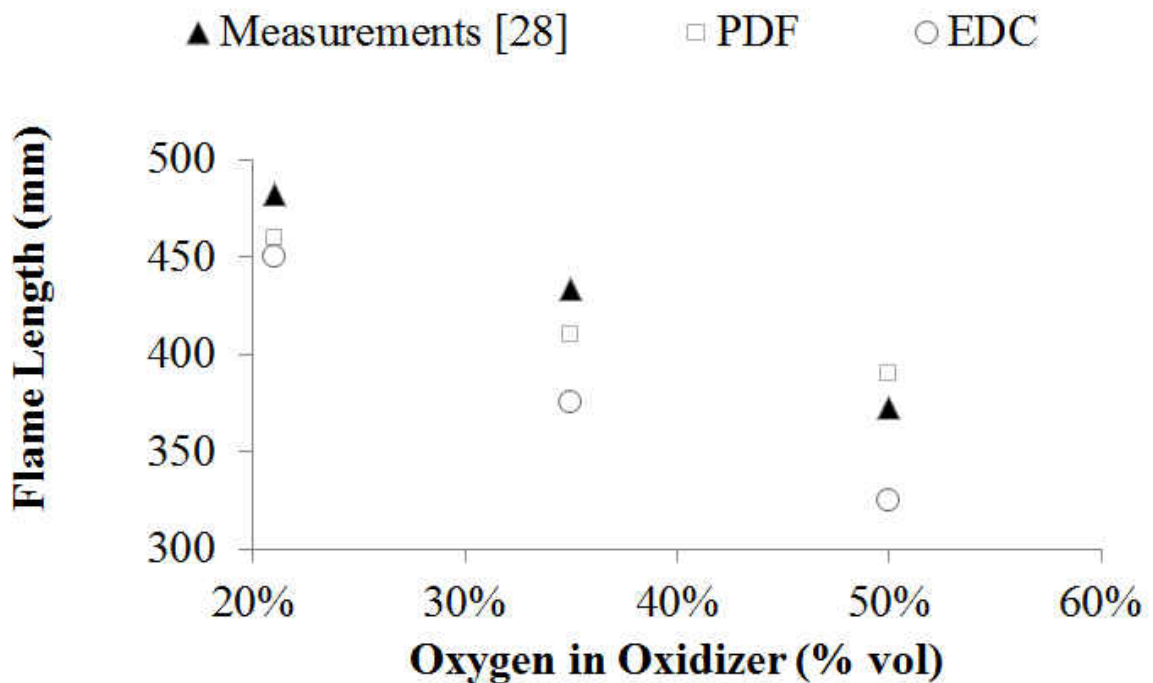


Figure 3-11: The sensitivity of flame length predictions to the choice of chemistry model for the air and oxy-flames investigated in this study.

Figure 3-12 shows the axial variation in the O radical concentrations in the three flames. Again, in accordance with the equilibria established by $O_2+H \leftrightarrow O+OH$, an

increase in the oxidizer O₂ concentration results in an increase in O radicals. Furthermore, in the EDC model the oxidation of CO was determined by the reactions: $\text{CO} + \text{OH} \leftrightarrow \text{CO}_2 + \text{H}$ and $\text{CO} + \text{O} + \text{M} \leftrightarrow \text{CO}_2 + \text{M}$. The second reaction is strongly exothermic and will therefore be favored at lower temperatures. Consequently, since the CO oxidation is dependent on the availability of OH and O radicals, it is interesting to note that the CO oxidation is limited to those flame residence times where OH and O are present and any unoxidized CO in the post-flame zone will remain so in the EDC model calculations. The reported trends in the OH concentrations reported in this study, confirm previous findings regarding pollutant formation that an increase in oxidation of soot through OH is expected in oxy-flames which was confirmed in our previous study of radiative transfer from these flames [22].

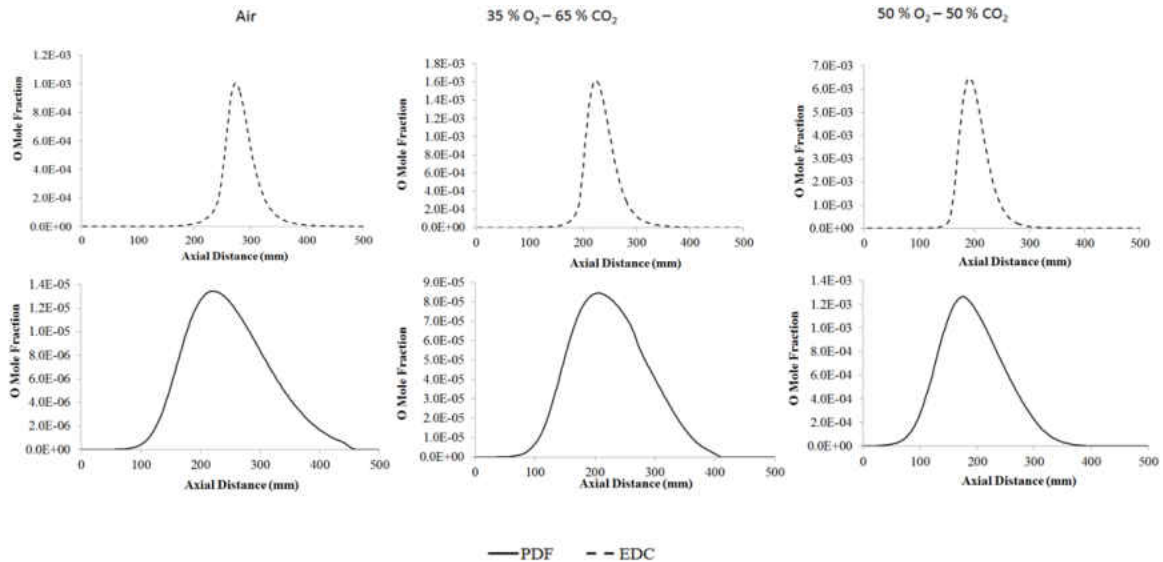


Figure 3-12: Axial O profiles for the air and oxy-flames investigated in this study.

3.4.6. Soret Effect

One of the shortcomings of the equilibrium PDF model is that it assumes equal species diffusivities and neglects thermophoresis (Soret effect) that might become important

when higher temperatures are encountered in the oxygen-enriched flames. While all the previously reported figures in this chapter accounted for Soret effect in the EDC calculations, Figure 3-13 compares the axial CO, OH and temperature variations in the three flames in the EDC model calculations with and without accounting for Soret effect in the calculations. The results indicate that with an increase in oxygen concentration in the oxidizer, the peak flame temperature increases and the flames get shorter. As a result, the temperature gradients increase and the Soret effect becomes more important in the oxy-flames. However, the Soret effect is seen to primarily affect only the peak concentrations and not the flame lengths. This is consistent with our previous findings where the flame length and radiant fraction predictions from employing the 41-step mechanism did not change as a result of including Soret effect even in an oxy-methane flame with 70% O₂ composition in the oxidizer where the highest temperatures were encountered.

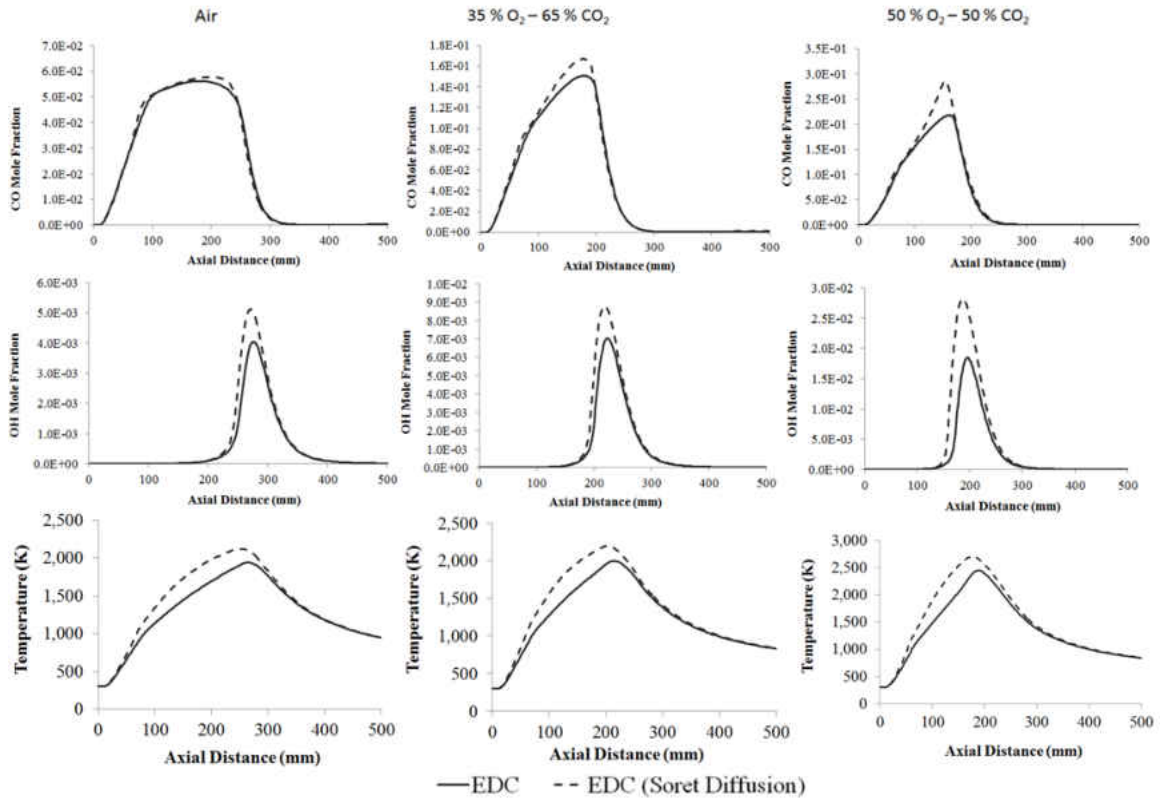


Figure 3-13: Axial CO, OH and temperature variations in the three flames in the EDC model calculations with and without accounting for Soret effect in the calculations.

3.5. Conclusions

Experimental measurements and computational fluid dynamic (CFD) simulations of three, confined, laminar (Re_{jet} 1404), diffusion, methane flames in oxidizer compositions of: 21% O_2 – 79% N_2 , 35 % O_2 - 65% CO_2 and 50% O_2 – 50 % CO_2 are reported in this study. The chemistry was modeled employing the Eddy Dissipation Concept (EDC) employing a 41-step detailed chemistry mechanism, the non-adiabatic extension of the equilibrium Probability Density Function (PDF) based mixture-fraction model and a two-step global finite rate chemistry model with modified rate constants proposed to work well under oxy-methane conditions. Based on the results from this study the following conclusions may be drawn:

1. Results from all the chemistry models were in reasonable agreement against the experimental measurements of O_2 , CO_2 and gas temperatures outside the flames at all oxidizer compositions. However, the CO predictions by the chemistry models were not that accurate. Although only the EDC model predicted CO in the fuel-lean regions outside the flame, the predictions were higher than the experimental measurements. This was likely a consequence of employing the EDC model in those localized regions outside the flames where the turbulent Reynolds number was less than 64. Moreover, variations in the centerline temperature predictions among the models were observed at lower axial locations.
2. The global finite rate chemistry model by virtue of limited dissociation predicted higher temperature than the PDF and EDC based approaches. The global finite rate chemistry model with the modified WD rate constants while predicting the CO_2 and O_2 concentrations well in the 35 % O_2 – 65 % CO_2 oxy-flame, deviates from their measured values in the 50 % O_2 – 50 % CO_2 oxy-flame. This is likely due to the fact that the refined kinetic parameters employed in the global finite rate chemistry model have been validated for highly turbulent scenarios and not for the laminar or laminar to transitional flames that were investigated in this study.
3. However, predictions from all 3 models in general are similar at large residence times in the post-flame zone when all of the combustion products attain equilibrium as well as in the fuel lean regions outside the flame. Furthermore, all models qualitatively predicted increase in CO concentrations with an increase in oxidizer CO_2 concentrations as observed in previous studies.

4. In contrast to previous studies, the CO predictions from all three chemistry models in these flames do not agree well against experimental measurements. This is probably attributed to the longer flame residence times and lower CO concentrations encountered in these flames. However, all three models qualitatively predicted increase in CO concentrations with an increase in oxidizer CO₂ concentrations.
5. Both the EDC and equilibrium PDF models correctly predicted increases in OH and O concentrations with increase in oxygen concentration in the oxidizer. When flame lengths were determined by the axial OH concentrations, the equilibrium PDF model predictions agreed more closely with experimental observations compared to those from the EDC model.
6. An investigation into the importance of the Soret diffusion revealed that thermophoresis has an effect on the flame temperature and peak OH and CO concentrations in the fuel rich regions. As anticipated its impact increases with an increase in peak flame temperatures and decrease in flame lengths that is associated with an increase in oxidizer oxygen concentrations. However, it does not have a significant impact on the flame length predictions.

Based on the results from this study the use of the equilibrium PDF in conjunction with a high-fidelity non-gray model for the radiative properties of the gas-phase may be deemed as accurate to capture the major gas species concentrations, temperatures and flame lengths in oxy-methane flames with long chemical residence times whereas detailed chemistry mechanisms with Soret effect need to be developed/validated to accurately predict pollutant concentrations such as CO, NO_x and soot.

3.6. References

- [1] P. Glarborg, L.L.B. Bentzen, Chemical effects of a high CO₂ concentration in oxy-fuel combustion of methane, *Energy & Fuels* 22 (2007) 291–6.
- [2] A. Amato, B. Hudak, P. D’Souza, P. D’Carlo, D. Noble, D. Scarborough, J. Seitzman, T. Lieuwen, Measurements and analysis of CO and O₂ emissions in CH₄/CO₂/O₂ flames, *Proceedings of the Combustion Institute* 33 (2011) 3399–3405.
- [3] F.S. Liu, H.S. Guo, G.J. Smallwood, O.L. Gulder, The chemical effects of carbon dioxide as an additive in an ethylene diffusion flame: Implications for soot and NO_x formation, *Combustion and Flame* 125 (2001) 778–87.
- [4] K.C. Oh, H.D. Shin, The effect of oxygen and carbon dioxide concentration on soot formation in nonpremixed flames, *Fuel* 85 (2006) 615–24.
- [5] H. Watanabe, T. Marumo, K. Okazaki, Effect of CO₂ Reactivity on NO_x Formation and Reduction Mechanisms in O₂/CO₂ Combustion *Energy Fuels* 26 (2012) 938–51.
- [6] R. Johansson, K. Andersson, B. Leckner, H. Thunman, Models for gaseous radiative heat transfer applied to oxy-fuel conditions in boilers, *International Journal of Heat and Mass Transfer* 53 (2010) 220–30.
- [7] C. Yin, L.C.R. Johansen, L.A. Rosendahl, S.K. Kær, New weighted sum of gray gases model applicable to computational fluid dynamics (CFD) modeling of oxy-fuel combustion: derivation, validation, and implementation, *Energy & Fuels* 24 (2010) 6275–82.
- [8] G. Krishnamoorthy, A new weighted-sum-of-gray-gases model for oxy-combustion scenarios, *International Journal of Energy Research* 37 (2013) 1752-63.

- [9] T. Kangwanpongpan, F. H. França, R. Corrêa da Silva, P.S. Schneider, H. J. Krautz, New correlations for the weighted-sum-of-gray-gases model in oxy-fuel conditions based on HITEMP 2010 database, *International Journal of Heat and Mass Transfer* 55 (2012) 7419–33.
- [10] C.K. Westbrook, F.K. Dryer, Simplified Reaction Mechanisms for the Oxidation of Hydrocarbon Fuels in Flames, *Combustion Science and Technology* 27 (1981) 31–43.
- [11] W.P. Jones, R.P. Lindstedt, Global reaction schemes for hydrocarbon combustion, *Combustion and Flame* 73 (1988) 233–49.
- [12] J. Andersen, C.L. Rasmussen, T. Giselsson, P. Glarborg, Global combustion mechanisms for use in CFD modeling under oxy-fuel conditions, *Energy & Fuels* 23 (2009) 1379–89.
- [13] C. Yin, L.A. Rosendahl, S.K. Kær, Chemistry and radiation in oxy-fuel combustion: A computational fluid dynamics modeling study, *Fuel* 90 (2011) 2519–29.
- [14] S. Hjærtstam, F. Normann, K. Andersson, F. Johnsson, Oxy-fuel combustion modeling: performance of global reaction mechanisms, *Industrial Engineering and Chemistry Research* 51 (2012) 10327–37.
- [15] R. Prieler, M. Demuth, D. Spoljaric, C. Hochenauer, Evaluation of a steady flamelet approach for use in oxy-fuel-combustion, *FUEL* 118 (2014) 55-68.
- [16] M.A Nemitallah, M.A Habib, Experimental and numerical investigations of an atmospheric diffusion oxy-combustion flame in a gas turbine model combustor, *Applied Energy* 111 (2013) 401–15.

- [17] C. Galletti, G. Coraggio, L. Tognotti, Numerical investigation of oxy-natural-gas combustion in a semi-industrial furnace: Validation of CFD sub-models, *Fuel* 109 (2013) 445–60.
- [18] Z. Wheaton, D. Stroh, G. Krishnamoorthy, M. Sami, S. Orsino, P. Nakod, A Comparative study of gray and non-gray methods of computing gas absorption coefficients and its effect on the numerical predictions of oxy-fuel combustion, *Industrial Combustion – Journal of the IFRF Article Number 201302* (2013) 1–14.
- [19] K. Bhadraiah, V. Raghavan, Numerical simulation of laminar co-flow methane–oxygen diffusion flames: effect of chemical kinetic mechanisms, *Combustion Theory and Modelling* 15 (2010) 23-46.
- [20] G. Kim, Y. Kim, Y.J. Joo. Conditional moment closure for modeling combustion processes and structure of oxy-natural gas flame, *Energy & Fuels* 23 (2009) 4370-7.
- [21] B.A.V Bennett, Z. Cheng, R.W. Pitz, M.D. Smooke, Computational and experimental study of oxygen-enhanced axisymmetric laminar methane flames, *Combustion Theory and Modelling* 12 (2008) 497–527.
- [22] H. Abdul-Sater, G. Krishnamoorthy, An assessment of radiation modeling strategies in simulations of laminar to transitional, oxy-methane, diffusion flames, *Applied Thermal Engineering* 61 (2013) 507–18.
- [23] M. Ditaranto, T. Oppelt, Radiative heat flux characteristics of methane flames in oxy-fuel atmospheres, *Experimental Thermal and Fluid Science* 35 (2011) 1343-50.
- [24] ANSYS FLUENT User’s Guide, Version 12, ANSYS Inc., Canonsburg, PA, 2009.
- [25] G. Krishnamoorthy, A New Weighted-sum-of-gray-gases model for CO₂-H₂O gas mixtures, *International Communications in Heat and Mass Transfer* 37 (2010) 1182–6.

- [26] A. De, E. Oldenhof, P. Sathiah, D.J.E.M. Roekaerts, Numerical simulation of delft-jet in-hot-coflow (DJHC) flames using the eddy dissipation concept model for turbulence-chemistry interaction, *Flow Turbul Combust* 87 (2011) 537–67.
- [27] A. Shiehnejadhesar, R. Mehrabian, R. Scharler, G.M. Goldin, I. Obernberger, Development of a gas phase combustion model suitable for low and high turbulence conditions, *Fuel* 126 (2014) 177-87.
- [28] M.D. Smooke, Reduced kinetic mechanisms and asymptotic approximation for methane–air flames: a topical volume. *Lecture Notes in Physics* vol. 384. Berlin: Springer-Verlag, (1991).
- [29] M. De Leo, A. Saveliev, L.A. Kennedy, S.A. Zelepouga, OH and CH luminescence in opposed flow methane oxy-flames, *Combustion and Flame* 149 (2007) 435–47.

4. PREDICTING RADIATIVE HEAT TRANSFER IN OXY-METHANE FLAME SIMULATIONS: AN EXAMINATION OF ITS SENSITIVITIES TO CHEMISTRY AND RADIATIVE PROPERTY MODELS

ABSTRACT

To account for the thermal and chemical effects associated with the high CO₂ concentrations in an oxy-combustion atmosphere, several refined gas-phase chemistry and radiative property models have been formulated and validated for laminar to highly, turbulent systems. However, significant turbulent interactions, “emission only” radiation modeling assumptions or the range of temperatures that were encountered in previous studies could have masked the variations that could potentially arise among these models predictions. This is demonstrated in this study by examining the variations in radiative transfer predictions due to the choice of chemistry and gas-phase radiative property models employed in computational fluid dynamic (CFD) simulations of laminar to transitional oxy-methane flames.

The gas-phase chemistry was modeled employing: a mixture-fraction based approach, the Eddy Dissipation Concept (EDC) and global finite rate chemistry models. The radiative properties were estimated employing four weighted-sum-of-gray-gases models (WSGGM) that were formulated employing different spectroscopic/model databases.

An average variation of 14 – 17% in the wall incident radiative fluxes was observed

between the EDC and equilibrium mixture fraction chemistry models, due to differences in their temperature predictions within the flame. One-dimensional, line-of-sight radiation calculations showed a 15 – 25 % reduction in the directional radiative fluxes at lower axial locations as a result of ignoring radiation from CO and CH₄. Under the constraints of fixed temperature and species distributions, the flame radiant power estimates and average wall incident radiative fluxes varied by nearly 60% and 11% respectively among the different WSGG models.

4.1. Introduction

4.1.1. Chemistry and Radiative Heat Transfer in Oxy-Methane Combustion

Furthermore, the increase in concentration of the radiatively participating gases (primarily CO₂ and H₂O but also CO as shown above) in an oxy-combustion medium can cause significant changes to the radiation characteristics within the furnace. Therefore, besides matching the flame temperature encountered during air-combustion, the need to match the corresponding wall radiative fluxes will also impact the determination of the optimum flue gas recycle ratios and oxidizer O₂ concentrations.

Similarly, refined WSGG models for the gas-phase radiative properties were determined to be necessary to accurately model radiative transfer. However, many of the studies were carried out in laminar systems employing an “emission only” radiation modeling assumption or in turbulent, semi-industrial scale systems with significant interactions between the chemistry, turbulence and radiative heat transfer. Furthermore, the range of temperatures encountered in these studies could have masked the variations that could potentially arise among the variation modeling options that have been deemed to be

appropriate for oxy-combustion scenarios.

4.1.2. Assessing the Accuracies of Radiative Transfer Predictions: Current Needs

The goal of this study is to assess the variations in the radiative transfer predictions as a result of employing different modeling options in oxy-methane combustion simulations. This is undertaken by: employing three of the chemistry models that have been deemed to be appropriate for simulating the combustion chemistry (cf. Table 3-1), minimizing the influences of particle radiation, turbulence-chemistry and turbulence-radiation interactions (TRI), examining the sensitivities to the spectroscopic database employed in the WSGGM formulations and quantifying the impacts of CO and CH₄ in the radiative transfer predictions. These are elaborated below:

1. In the laminar flow experiments listed in Table 3-1 although the temperature and concentrations of the radiatively participating species were well resolved, the radiative transfer calculations were carried out employing the optically thin radiation model. Under the optically thin assumption, each radiating point source within the flame has an unimpeded, isotropic view of its cold surroundings. The radiative loss rate per unit volume of the determined as a function of the absorption coefficient and the difference between the fourth powers of the local flame temperature and the cold surrounding temperature. While this is generally a good assumption in open flames where radiation is not the dominant heat transfer mechanism, this approximation is not valid in enclosed flames where radiative heating of the walls and radiation from the combustion gases within the enclosure are important. Furthermore, the wall/surface radiative heat fluxes

cannot be determined when employing the optically thin radiation model in these scenarios as a rigorous solution to the radiative transfer equation (RTE) is not being undertaken.

To address this need, experimental measurements from confined, laminar (Re 1404), methane flames in oxidizer compositions of: 21% O_2 - 79 % N_2 , 35 % O_2 – 65% CO_2 and 50% O_2 – 50% CO_2 are first reported in this study, followed by computational fluid dynamic (CFD) simulations of these flames employing the discrete ordinates radiation model. The results reported therefore include wall radiative fluxes in an environment where turbulence-radiation interactions (TRI) were also minimized [1]. The importance of TRI was recognized in a recent study carried out by Becher et al. [2] where significant TRI precluded the determination of the most accurate radiative property model. Furthermore, as noted in Table 3-1, most of the investigated oxy-methane combustion systems were turbulent and at a semi-industrial scale where a significant inter-play between the turbulence, chemistry and radiative heat transfer were likely prevalent.

2. The different WSGGM formulations for oxy-combustion scenarios have been undertaken employing different spectroscopic/model data bases. For instance, Johansson et al [3] employed the EM2C statistical narrow band model (SNB), Yin et al. [4] the exponential wide band model (EWBM), Krishnamoorthy [5] employed the RADCAL SNB and Kangwanpongan [6] the HITEMP 2010 spectroscopic databases. While all the above-referenced models were validated through comparisons against benchmark/line-by-line (LBL) data for prototypical problems [5 – 7] at temperatures less than 1800 K, significant variations among the underlying spectroscopic databases employed in their

formulation can result in corresponding variations in the radiative transfer predictions in coupled combustion calculations where strong variations in the $\text{H}_2\text{O}/\text{CO}_2$ ratios are observed and the flame temperature greatly exceeds 1800 K. For instance, Lallemand et al. [8] observed a significant variation in the emissivity predictions due to the differences in spectroscopic/model databases employed in the emissivity calculations.

Recently, a similar evaluation at conditions representative of oxy-combustion scenarios was carried out by Becher et al [9], however at constant $\text{H}_2\text{O}/\text{CO}_2$ ratios and constant temperature conditions (800 K – 1800 K). By comparing, the total emissivities predicted by different WSGG model formulations against those obtained from the HITEMP 2010 spectroscopic database, they determined the WSGGM formulation of Johansson et al [10] to be the most versatile and computationally efficient model, followed by the older model of Johansson et al [3]. A comparison against the updated WSGGM parameters based on the RADCAL SNB that was published in Krishnamoorthy et al [5] was not carried out likely due to the close timing of both these publications. However, in a more recent study Kangwanpongpan et al. [6] published WSGGM correlations based on fitting the coefficients to total emissivities from the HITEMP 2010 LBL database. In their study, the radiative heat fluxes and its divergence were obtained from LBL calculations for test cases encompassing wide ranges of composition non-homogeneities, non-isothermal media and path lengths and were treated as benchmarks. Their proposed WSGGM was then demonstrated to be the most accurate formulation when compared against the benchmark with large errors associated with the EM2C SNB based model of Johansson et al [10]. The laminar oxy-methane flames in enclosed environments (such as those examined in this study) as a result of the oxygen enriched

combustion environment can attain local temperatures greater than 2400 K within the flame and by virtue of their shorter flame lengths, encounter sharper temperature and species concentration gradients as well as result in volume-averaged reactor temperatures that are much lower than 800 K. Since these extremes are well outside the range of conditions examined in the studies of Becher et al. [9] and Kangwanpongpan et al. [6], it is worthwhile to examine the radiative transfer variations that might result from employing different WSGGM formulations, in particular when validation against experimental data from these flames is being attempted.

Therefore in this study, radiative heat transfer calculations were performed by estimating the gas-phase radiative properties of H₂O and CO₂ employing different WSGGM for oxy-combustion scenarios that were formulated employing four different spectroscopic databases [3-6]. All of the WSGGM were implemented as User-Defined Functions (UDFs) and employed in conjunction with the CFD code ANSYS FLUENT [11]. In addition, the modeling of the gas-phase chemistry was undertaken employing the non-adiabatic extensions of the equilibrium Probability Density Function (PDF) based mixture-fraction model, a two-step global finite rate chemistry model with modified rate constants and the Eddy Dissipation Concept (EDC) employing a 41-step detailed chemistry mechanism, models that have been deemed to be acceptable in oxy-combustion scenarios as listed in Table 3-1.

3. All of the proposed WSGGM formulations [3 – 6] only account for the varying H₂O/CO₂ concentrations in the medium while calculating the radiative properties but neglect the participation of CO and CH₄ in radiative heat transfer. However, as previously noted, high CO concentrations are present in the near-burner region during oxy-combustion that

can impact the flame heat loss and the burner/wall radiative fluxes and temperatures. Subsequently, these can have a strongly influence on the flame stability and lift-off characteristics [12]. Therefore, the contributions of CO and CH₄ in the radiative transfer need to be properly assessed. To address this, the SNB RADCAL [13] was employed to perform one-dimensional radiative transfer calculations to assess the contributions of CO and CH₄ to the radiative fluxes in these flames.

4.2. Experimental Conditions

For a complete description of the experimental conditions, the reader is referred to section 3.2 of this thesis and to Ditaranto et al [14]

4.3. CFD Modeling Approach

4.3.1. Mesh and Flow Modeling

The modeling strategy and mesh is fully described in section 3.3.1.

4.3.2. Radiation Modeling and Boundary Conditions

In order to investigate the sensitivity of the predictions to the spectroscopic/model databases alone employed in the WSGGM formulations, additional radiative transfer calculations were carried out by “freezing” the converged flow field that was obtained with the SNB RADCAL based WSGGM. This was made to ensure that all the WSGGM calculations were performed on the same temperature and specie concentration fields and any differences in the radiative source term predictions across the models do not translate to any further changes to the thermal field that can further magnify/minimize the differences in the radiative transfer predictions among the models. The different WSGGM investigated in this study along with their model notations employed in this study, the number of gray-gases

(gg) and the spectroscopic data bases associated with their formulation are listed in Table 4-1.

Table 4-1: A summary of WSGGM investigated in this study

Model Notation (Number of gray gases)	Spectroscopic database	Reference
Perry (5 gg)	SNB RADCAL, Perry's Chemical Engineering Handbook	5
EM2C (5 gg)	EM2C SNB	3
EWBM (5 gg)	EWBM	4
HITEMP 2010 (5 gg)	HITEMP 2010	6

4.3.3. Chemistry Modeling

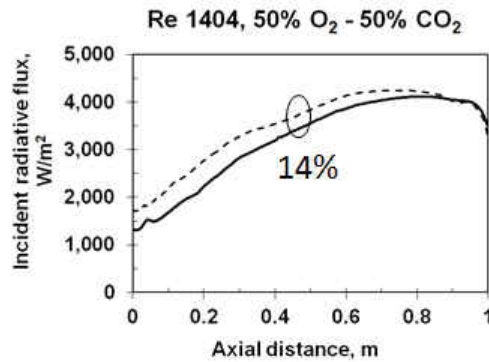
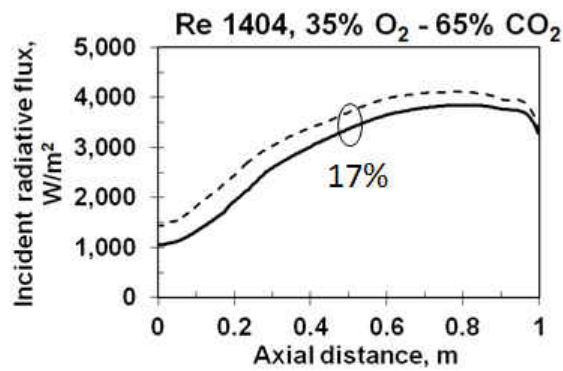
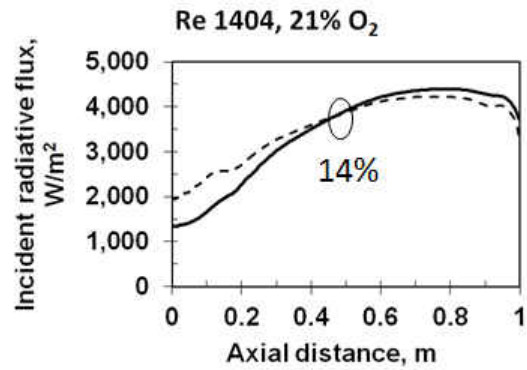
Based on the recent studies summarized in Table 3-1, it is evident that the non-adiabatic extension of the equilibrium PDF based mixture-fraction model, the Eddy Dissipation Concept (EDC) and global finite rate chemistry (FR) have been deemed to be appropriate for simulating the laminar to transitional oxy-methane flames investigated in this study. Therefore, simulations employing all three models were employed in this study to examine the variations in radiative transfer.

4.4. Results and Discussion

4.4.1. Wall Incident Radiative Fluxes

Since the EDC and PDF models account for dissociation and radical concentrations, the variations in the incident radiative fluxes (in W/m^2) at the wall predicted from employing these two chemistry models in the simulations are shown in Figure 4-1. The wall averaged

percentage variations among the models are indicated near circled regions. The gas phase radiative properties were all determined using the Perry (5 gg) WSGGM. Since higher flame temperatures are predicted by the EDC model (cf. Figure 3-1 to Figure 3-3), the wall incident radiative fluxes are also higher by 14 – 17 % across all flames.



— PDF - - EDC

Figure 4-1: Variations in the incident radiative fluxes (in W/m²) at the wall predicted by the different chemistry models (the wall averaged percentage variations between the models are indicated near circled regions).

4.4.2. Directional Radiative Flux Predictions from RADCAL

RADCAL [15] is a narrow band model that adopts the Curtis-Godson approximation together with the single line group (SLG) model [16] to compute the spectral intensities from a non-isothermal mixture of combustion gases (CO, CO₂, H₂O and CH₄) and soot, incident upon a volume element. Collision and Doppler broadened optical depths are first computed in the calculations and then combined to calculate an overall optical depth. The contributions from all the species to the total spectral optical depth are assumed to be additive. However, the user has the option to selectively turn off the radiation contribution from any specie. The spectral transmittance and spectral intensity are then obtained from the overall optical depth by solving the radiative transfer equation (RTE) along the line of sight. Details of this calculation procedure can be found in Grosshandler [15] and Ludwig et al. [16]. For performing the RADCAL calculations, the CO, CO₂, H₂O and CH₄, Temperature profiles at different axial locations in the three flames (Re 1404) were exported from the CFD calculations into a form readable by RADCAL. Figure 4-2, compares the directional radiative flux (in W/m²-Sr) at different elevations along the furnace wall. The chemistry model that was employed to determine the specie and temperature fields are indicated in the legends. At lower axial locations, higher directional radiative fluxes are predicted by the FR model by virtue of their higher centerline temperature predictions (cf. Figure 3-1 to Figure 3-3). However, the directional radiative flux predictions from all three chemistry models converge to approximately the same values at higher axial locations analogous to what was observed with the temperature fields in Figure 3-1 to Figure 3-3. The directional radiative fluxes also increase with an increase oxygen concentration in the oxidizer stream due to higher centerline temperatures. The open symbols in Figure 4-2 represent the calculations

where the contributions of CO and CH₄ to the radiative transfer were not accounted for in RADCAL. As anticipated CO and CH₄ radiation contributions are maximum at lower axial locations at their highest concentrations (and temperatures) and their contributions quickly become negligible at higher axial locations. These effects are further quantified in Figure 4-3 where the percentage reduction in the directional radiative flux when not accounting for both CO and CH₄ radiation are shown for fuel Reynolds numbers in the range 468 to 2340. A maximum of 15 % reduction in the directional radiative fluxes at the walls is observed at lower axial locations as a result of ignoring the participation of both CO and CH₄ in the radiation calculations as done in all of the proposed WSGGM formulations. The global FR chemistry model by virtue of predicting higher centerline temperatures also predicts a greater CO, CH₄ contribution to the flame radiation (up to 25 % in the methane-air flame at lower axial locations). The individual contributions of CO and CH₄ to the radiative transfer were determined to be roughly equal in these flames. Radiation from CO and CH₄ in the near burner region can therefore impact the flame stability and lift-off characteristics in these flames.

In spite of the increases in CO concentrations and temperatures in the oxy-flames, the corresponding increase in the combined concentrations of CO₂ and H₂O minimizes the relative importance of radiation from CO and CH₄. However, with an increase in fuel Reynolds numbers the contributions of CO and CH₄ to the radiative transfer are seen to be clearly prevalent to greater axial heights.

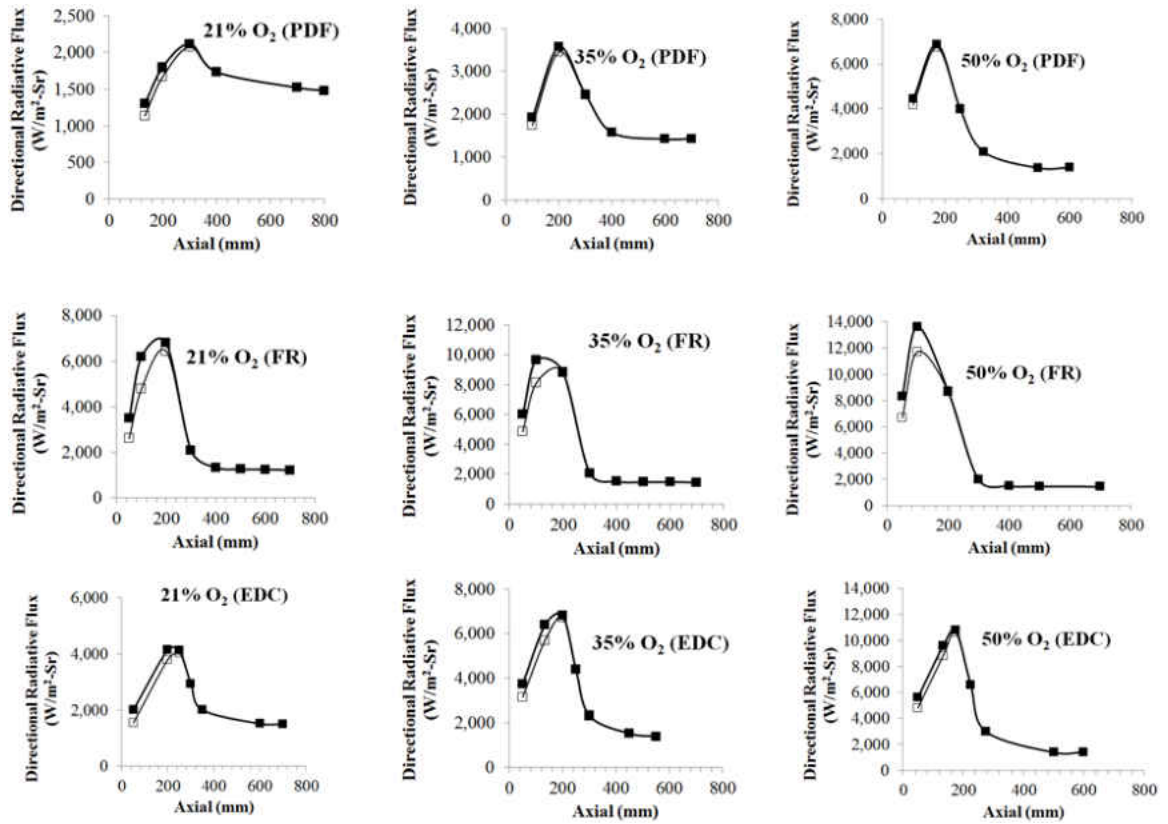
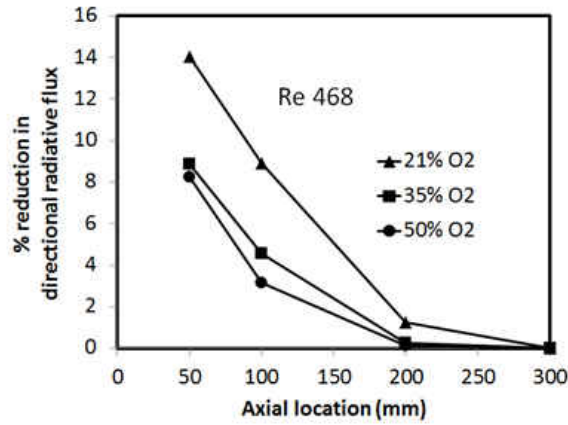
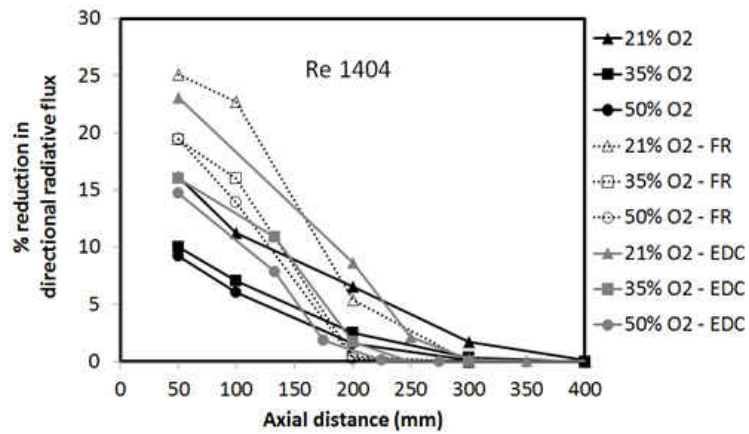


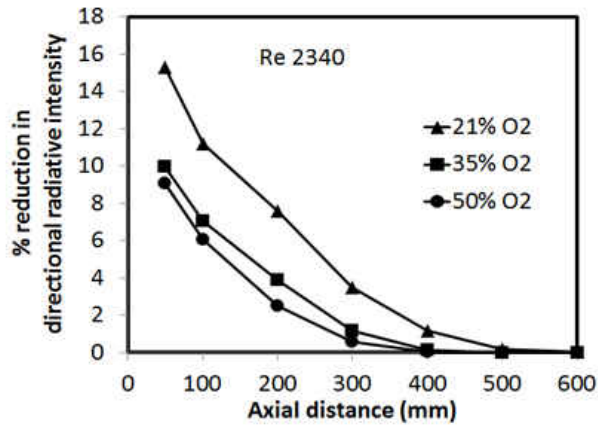
Figure 4-2: Directional radiative flux predictions from RADCAL at different heights along the furnace wall in the air and oxy-flames flames (Re 1404). Open symbols correspond to predictions where CO, CH₄ radiation was not accounted for in the calculations.



(a)



(b)



(c)

Figure 4-3: Percentage reduction in the directional radiative flux when not accounting for CO, CH₄ contributions to radiative transfer in calculations performed with mixture fraction based chemistry model (unless indicated in the legends) and Perry (5gg) WSGGM: (a) Re 468; (b) Re 1404; (c) Re 2340.

4.4.3. Effect of WSGGM Spectroscopic/Model Database

The radiative source term describes the conservation of radiative energy within a control volume and goes into the total energy equation, thereby coupling radiation with the other physical processes that occur in a multi-physics application. If “k” represents the absorption coefficient within a control volume, “G” the total incident radiation and I_b the black body emissive power, then the radiative source term $-\nabla \cdot \mathbf{q}(\mathbf{r})$ can be computed by summing the contributions over all bands “i” as:

$$-\nabla \cdot \mathbf{q}(\mathbf{r}) = \sum_{i=\text{band}} k_i(\mathbf{r})(G_i(\mathbf{r}) - 4\pi I_{b,i}(\mathbf{r})) \quad \text{Equation 4-1}$$

G_i , the incident radiation in Equation 4-1 is calculated by integrating the directional intensities (I) associated with the wavelength band “i” over all directions as:

$$G_i(\mathbf{r}) = \int_{4\pi} I_i(\mathbf{r}, \hat{\mathbf{s}}) d\Omega \quad \text{Equation 4-2}$$

A negative value of the radiative source term corresponds to a net emission. The volume integral of the radiative source term therefore is a measure of the total radiative energy lost by the flame as a result of emission and absorption and is therefore employed to determine the flame radiant fractions (by dividing the volume integral of Equation 4-2 by the product of fuel heating value and mass flow rate). Table 4-2 compares the volume integrated radiant source (or the magnitude of radiant power) predicted by the different WSGGM. The volume integrated radiant source was computed as:

$$Q_R = -\iiint_V \nabla \cdot \mathbf{q}(\mathbf{r}) dV \quad \text{Equation 4-3}$$

Also shown in Table 3 are the average $\text{H}_2\text{O}/\text{CO}_2$ ratios in the domain and the

maximum percentage variation in Q_R . The maximum percentage variation for each flame was computed as:

$$\frac{Q_{R,high} - Q_{R,low}}{Q_{R,high}} \times 100 \quad \text{Equation 4-4}$$

Table 4-2: Volume integrated radiative source (in W) (Q_R) for the different flames investigated in this study.

21 % O2						
	EWBM (5 gg)	Perry (5 gg)	EM2C (5 gg)	HITEMP 2010 (5 gg)	Max % variation	H2O/CO2
Re 468	-93	-106	-136	-146	-57	1.99
Re 1404	-801	-753	-885	-1087	-44	2.00
Re 2340	-1871	-1889	-2050	-2507	-34	2.00

35 % O2						
	EWBM (5 gg)	Perry (5 gg)	EM2C (5 gg)	HITEMP 2010 (5 gg)	Max % variation	H2O/CO2
Re 468	-131	-129	-150	-138	-16	0.04
Re 1404	-740	-723	-1184	-787	-64	0.11
Re 2340	-2049	-1723	-2792	-2199	-62	0.17

50 % O2						
	EWBM (5 gg)	Perry (5 gg)	EM2C (5 gg)	HITEMP 2010 (5 gg)	Max % variation	H2O/CO2
Re 468	-133	-127	-147	-134	-16	0.05
Re 1404	-813	-781	-1271	-840	-63	0.14
Re 2340	-2146	-1794	-2841	-2233	-58	0.22

Significant variation (up to 60%) in Q_R is observed in both the air and oxy-flames. Figure 4-4 shows the variations in the incident radiative fluxes along the walls of the furnace (in the axial direction). The wall incident radiative fluxes were determined through an integration of the normal component of the directional intensities over a hemi-sphere as:

$$\mathbf{q}(\mathbf{r}) = \int_{4\pi} I(\mathbf{r}, \hat{\mathbf{s}}) \hat{\mathbf{s}} d\Omega \quad \text{Equation 4-5}$$

The maximum of the wall averaged percentage variations between the models are also indicated near circled region. To determine this, the maximum percentage variation among the models was computed at each computational cell along the wall (i.e., by employing $\mathbf{q}(\mathbf{r})$

in Equation 4-4) and averaged over all cells along the wall.

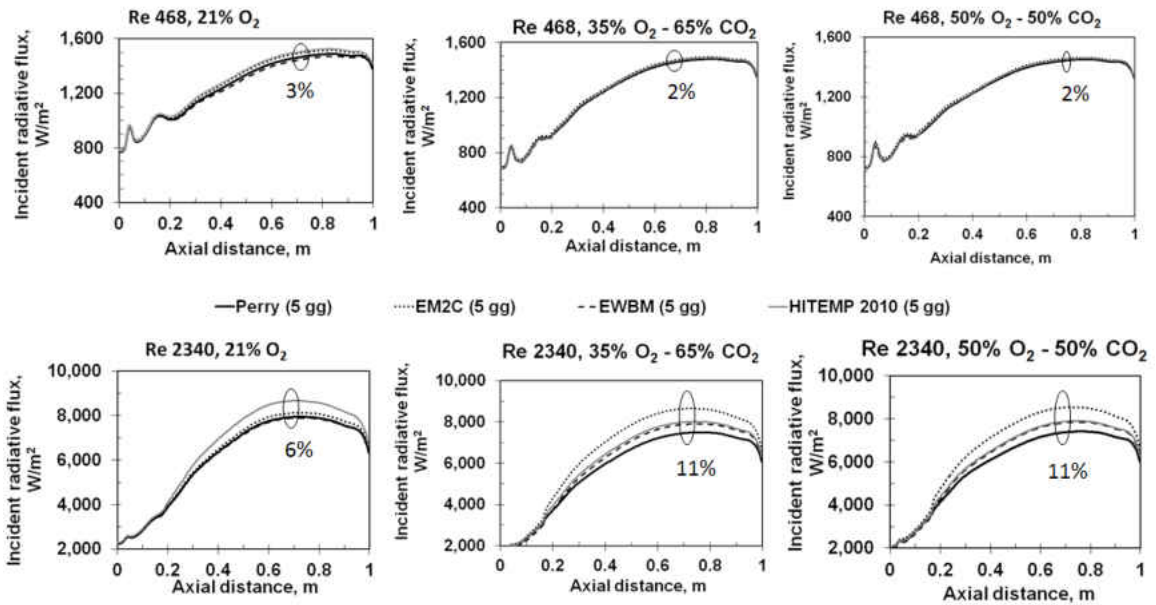


Figure 4-4: Variations in the incident radiative fluxes (in W/m²) at the wall predicted by the different WSGG models (the maximum of the wall averaged percentage variations between the models are indicated near circled regions).

Wheaton et al [17] had previously examined the variations in the wall incident radiative flux predictions as a result of employing the EM2C (5 gg) and Perry (5 gg) in the model calculations. In their study, although high concentrations of radiatively participating gases were present, the average H₂O/CO₂ ratio within the turbulent furnaces was approximately 2 (close to the air-methane flames in this study). This ratio resulted from the fact that the simulations were of: oxygen-enriched combustion without flue gas recirculation in one system and high temperature air combustion where there was a large amount of wet flue gas recirculation. Although temperatures greater than 1800 K were encountered in those systems as well, the nearly homogeneous, isothermal conditions encountered within those systems along with the EM2C (5 gg) and Perry (5 gg) WSGGM compared in that study showed no significant difference in radiative flux predictions arising from the choice of the

WSGGM model/spectroscopic database. It is worth noting in Figure 4-4 that the EM2C (5 gg) and the Perry (5 gg) model wall radiative flux predictions are nearly identical in methane-air flames. In contrast, this study shows that the variations among the WSGGM predictions may not always be negligible in air and oxy-fired systems.

4.5. Conclusions

The past few years have seen the development, refinement and validation of several chemistry and radiative property models for simulating oxy-methane combustion. However, many of the studies were carried out in laminar systems employing an “emission only” radiation modeling assumption or in turbulent, semi-industrial scale systems with significant interactions between the chemistry, turbulence and radiative heat transfer. Furthermore, the range of temperatures encountered in these studies could have masked the variations that could potentially arise among these models predictions. This is demonstrated in this study by examining the variations in radiative transfer predictions in oxy-methane flames in a system where: the influence of turbulence is minimized, and the discrete ordinates method was employed to solve the RTE. Three chemistry models and four radiative property models for the gas-phase, all of which have been deemed to be appropriate for simulating these scenarios were employed in the simulations.

The chemistry was modeled employing the non-adiabatic extension of the equilibrium Probability Density Function (PDF) based mixture-fraction model, the Eddy Dissipation Concept (EDC) employing a 41-step detailed chemistry mechanism, and a two-step global finite rate chemistry model with modified rate constants proposed to work well under oxy-methane conditions. The non-gray, gas-phase radiative properties of H₂O and CO₂

were determined employing different formulations of the weighted-sum-of-gray-gases models (WSGGM) that were based on four different spectroscopic/model databases. Based on the results from this study the following conclusions may be drawn:

1. The centerline temperature variations among the chemistry models were reflected in one-dimensional, line-of-sight calculations of the directional radiative flux at the walls carried out employing the statistical narrow band model RADCAL as well as in the incident radiative heat flux profiles obtained from discrete ordinates model simulations of radiative transfer. When employing the same WSGGM, an average variation of 14 – 17% in the wall incident radiative fluxes was observed between the EDC and equilibrium mixture fraction chemistry models, due to differences in their temperature predictions within the flame.
2. When employing the temperature and specie concentration fields obtained from the equilibrium mixture fraction model predictions, RADCAL calculations indicated a maximum of 15 % reduction in the directional radiative fluxes at the walls at lower axial locations as a result of ignoring the participation of both CO and CH₄ in the radiation calculations as done in all of the proposed WSGGM formulations. In spite of the increases in CO concentrations and temperatures in the oxy-flames, the corresponding increase in the combined concentrations of CO₂ and H₂O minimized the relative importance of radiation from CO and CH₄. However, with an increase in fuel Reynolds numbers the contributions of CO and CH₄ to the radiative transfer were clearly prevalent to greater axial heights. The global finite rate chemistry model by virtue of predicting higher centerline temperatures also predicted a greater CO, CH₄ contribution to the flame radiation (up to 25 % in the methane-air flame at lower axial locations). Radiation from

CO and CH₄ in the near burner region can therefore impact the flame stability and lift-off characteristics in these flames.

3. Under the constraint of a fixed temperature and species distributions obtained from equilibrium mixture fraction model simulations, differences in the spectroscopic/model databases employed in the WSGGM formulations resulted in a nearly 60% variation in the volume integrated radiative source term predictions (which is employed to estimate the flame radiative fraction) in all of the flames examined. In general, the variations increased with increase in flame lengths (i.e., with fuel Re) and flame temperatures (which were higher in the oxy-flames). These were also reflected in the variations in the wall incident radiative flux predictions among the models with the average variation among the WSGGM formulations increasing up to 11% in the Re 2340 oxy-flames.

4.6. References

- [1] H. Abdul-Sater, G. Krishnamoorthy, An assessment of radiation modeling strategies in simulations of laminar to transitional, oxy-methane, diffusion flames, *Applied Thermal Engineering* 61 (2013) 507–18.
- [2] V. Becher, J.P. Bohn, P. Dias, H. Spliethoff, Validation of spectral gas radiation models under oxyfuel conditions—part B: natural gas flame experiments, *Int. J. Greenhouse Gas Control* 5 (2011) S66–S75.
- [3] R. Johansson, K. Andersson, B. Leckner, H. Thunman, Models for gaseous radiative heat transfer applied to oxy-fuel conditions in boilers, *International Journal of Heat and Mass Transfer* 53 (2010) 220–30.

- [4] C. Yin, L.C.R. Johansen, L.A. Rosendahl, S.K. Kær, New weighted sum of gray gases model applicable to computational fluid dynamics (CFD) modeling of oxy–fuel combustion: derivation, validation, and implementation, *Energy & Fuels* 24 (2010) 6275–82.
- [5] G. Krishnamoorthy, A new weighted-sum-of-gray-gases model for oxy-combustion scenarios, *International Journal of Energy Research* 37 (2013) 1752-63.
- [6] T. Kangwanpongpan, F. H. França, R. Corrêa da Silva, P.S. Schneider, H. J. Krautz, New correlations for the weighted-sum-of-gray-gases model in oxy-fuel conditions based on HITEMP 2010 database, *International Journal of Heat and Mass Transfer* 55 (2012) 7419–33.
- [7] H. Chu, F. Liu, H. Zhou, Calculations of gas thermal radiation transfer in one-dimensional planar enclosure using LBL and SNB models, *Int. J. Heat Mass Transfer* 54 (2011) 4736-4745.
- [8] N. Lallemand, A. Sayre, R. Weber, Evaluation of emissivity correlations for H₂O–CO₂–N₂/air mixture and coupling with solution methods of the radiative transfer equation, *Progress in Energy and Combustion Science* 22 (1996) 543–74.
- [9] V. Becher, A. Goanta, H. Spliethoff, Validation of spectral gas radiation models under oxyfuel conditions–Part C: Validation of simplified models, *Int. J. Greenhouse Gas Control* 11 (2012) 34-51.
- [10] R. Johansson, B. Leckner, K. Andersson, F. Johnsson, Account for variations in the H₂O to CO₂ molar ratio when modelling gaseous radiative heat transfer with the weighted-sum-of-grey-gases model, *Combustion and Flame* 158 (2011), 893–901.
- [11] ANSYS FLUENT User’s Guide, Version 12, ANSYS Inc., Canonsburg, PA, 2009.

- [12] B.L. Norheim, Lift-off of methane jet flames in O₂/CO₂ atmospheres, MS Thesis Department of Energy and Process Engineering, Norwegian University of Science and Technology (2009).
- [13] W.L. Grosshandler, Radiative heat transfer in nonhomogeneous gases: a simplified approach, *International Journal of Heat and Mass Transfer* 23 (1980) 1447–59.
- [14] M. Ditaranto, T. Oppelt, Radiative heat flux characteristics of methane flames in oxy-fuel atmospheres, *Experimental Thermal and Fluid Science* 35 (2011) 1343-50.
- [15] W.L. Grosshandler, RADCAL: a narrow-band model for radiation calculations in a combustion environment, NIST Technical Note, 1402 (1993).
- [16] C.B. Ludwig, W. Malkmus, J.E. Reardon, and J.A.L. Thomson (eds. R. Goulard and J.A.L. Thomson), *Handbook of infrared radiation*, Washington, DC: NASA SP-3080 (1973).
- [17] Z. Wheaton, D. Stroh, G. Krishnamoorthy, M. Sami, S. Orsino, P. Nakod, A Comparative study of gray and non-gray methods of computing gas absorption coefficients and its effect on the numerical predictions of oxy-fuel combustion, *Industrial Combustion – Journal of the IFRF Article Number 201302* (2013) 1–14.

5. CONCLUSIONS

A comprehensive assessment was carried out in this thesis to determine the accuracies of CFD simulations using different chemistry and radiation modeling procedures. The effects and sensitivities of radiative heat transfer predictions to three chemistry models were also investigated. Laminar to transitional, air-methane and oxy-methane diffusion flames in a lab-scale furnace were chosen to minimize the impact of the turbulence modeling procedure and the uncertainties associated with the particle contribution to radiation. This thesis is divided into three sections: 1) an investigation into the effects of gray and non-gray radiation modeling on variables important to radiative heat transfer, 2) an investigation on the impact of several chemistry models on temperature and other variables and 3) an assessment on the sensitivities of radiative heat transfer predictions to the choice of radiation and chemistry models.

5.1. Summary of Results

In Chapter 2, combustion chemistry was modeled using the non-adiabatic extension of the equilibrium based mixture fraction model. The radiation models used were gray and non-gray formulations of the Perry model. Predictions of gas, wall temperatures and flame lengths were in good agreement with experimental measurements. The temperature and flame length predictions were not sensitive to the radiative property model employed. There

were significant variations between the gray and non-gray model radiant fraction predictions with the variations in general increasing with decrease in Reynolds numbers possibly attributed to shorter flames and steeper temperature gradients. The inclusion of soot model and TRI model did not affect our predictions as a result of low soot volume fractions and the radiation emission enhancement to the temperature fluctuations being localized to the flame sheet

In Chapter 3, CFD simulations of and experimental results from three laminar, diffusion methane flames in oxidizer compositions of: 21% O₂ – 79% N₂, 35 % O₂ - 65% CO₂ and 50% O₂ – 50 % CO₂ were reported. The non-gray radiation model for the radiative properties of the gas-phase was employed for all simulations. The chemistry was modeled employing the Eddy Dissipation Concept (EDC) employing a 41-step detailed chemistry mechanism, the non-adiabatic extension of the equilibrium Probability Density Function (PDF) based mixture-fraction model and a two-step global finite rate chemistry model with modified rate constants proposed to work well under oxy-methane conditions. Based on the results from this chapter, employing the non-gray model for the radiative properties of the gas-phase in conjunction with the equilibrium PDF chemistry model may be deemed accurate to capture the major species concentrations, temperatures and flame lengths in oxy-methane flames with long chemical residence times whereas detailed chemistry mechanisms with Soret effect need to be developed/validated to accurately predict pollutant concentrations such as CO, NO_x and soot.

Chapter 4 examined the variations in radiative transfer predictions in oxy-methane flames in a system where the influence of turbulence was minimized. Three chemistry models and four radiative property models for the gas-phase were employed in the

simulations of the flames investigated in Chapter 3. The non-gray, gas-phase radiative properties of H₂O and CO₂ were determined employing different formulations of the weighted-sum-of-gray-gases models (WSGGM) that were based on four different spectroscopic/model databases. The results showed that an average variation of 14 – 17% in the wall incident radiative fluxes was observed between the EDC and equilibrium mixture fraction chemistry models due to differences in their temperature predictions within the flame. The increases in CO concentrations and temperatures in the oxy-flames and the corresponding increase in the combined concentrations of CO₂ and H₂O minimized the relative importance of radiation from CO and CH₄. However, with an increase in fuel Reynolds numbers the contributions of CO and CH₄ to the radiative transfer were clearly prevalent to greater axial heights. One-dimensional, line-of-sight radiation calculations showed a 15 – 25 % reduction in the directional radiative fluxes at lower axial locations as a result of ignoring radiation from CO and CH₄. Under the constraints of fixed temperature and species distributions, the flame radiant power estimates and average wall incident radiative fluxes varied by nearly 60% and 11% respectively among the different WSGG models.

5.2. Future Work

Future work will investigate the sensitivities of flame lift-off heights to the choice of gas-phase chemistry and radiation sub-models. Flame lift-off predictions from methane flames at various co-flow and oxidizer conditions will be compared to experimental measurements. A preliminary investigation on lift-off predictions in the flames considered in this thesis revealed the necessity for improved predictions of CO. As discussed in section 3.4.4, an improved agreement in CO predictions may be obtained by the hybrid model or by

employing a more detailed chemistry mechanism.